Structural Engineering and Mechanics, *Vol. 68, No. 1 (2018) 103-119*
DOI: https://doi.org/10.12989/sem.2018.68.1.103

A nonlocal strain gradient theory for nonlinear free and forced vibration of embedded thick FG double layered nanoplates

E. Mahmoudpour[1], SH. Hosseini-Hashemi[*2a] and S. A. Faghidian[1a]

[1]*Department of Mechanical Engineering, Science and Research Branch, Islamic Azad University, Tehran, Iran*
[2]*School of Mechanical Engineering, Iran University of Science and Technology, Tehran, Iran*

(Received April 9, 2018, Revised July 12, 2018, Accepted July 21, 2018)

Abstract. In the present research, an attempt is made to obtain a semi analytical solution for both nonlinear natural frequency and forced vibration of embedded functionally graded double layered nanoplates with all edges simply supported based on nonlocal strain gradient elasticity theory. The interaction of van der Waals forces between adjacent layers is included. For modeling surrounding elastic medium, the nonlinear Winkler-Pasternak foundation model is employed. The governing partial differential equations have been derived based on the Mindlin plate theory utilizing the von Karman strain-displacement relations. Subsequently, using the Galerkin method, the governing equations sets are reduced to nonlinear ordinary differential equations. The semi analytical solution of the nonlinear natural frequencies using the homotopy analysis method and the exact solution of the nonlinear forced vibration through the Harmonic Balance method are then established.

The results show that the length scale parameters give nonlinearity of the hardening type in frequency response curve and the increase in material length scale parameter causes to increase in maximum response amplitude, whereas the increase in nonlocal parameter causes to decrease in maximum response amplitude. Increasing the material length scale parameter increases the width of unstable region in the frequency response curve.

Keywords: nonlinear vibration; FG double layered nanoplate; nonlocal strain gradient theory; homotopy analysis method; nonlinear elastic medium

1. Introduction

Nanotechnology is employed in many scientific fields. Graphene sheet (GS) is one of famous element in nanostructures. GSs are defined as one-atom-thick of carbon layers tightly packed into a honeycomb lattice. The analysis of GSs is a basic issue in the investigation of carbon nano-materials. The amazing electrical and mechanical properties such as flexibility, low thermal expansion and high electrical conductivity made them to use in nanostructured materials. In order to reinforcement of polymer composites the GSs are often used as embedded structures. Since the bending modulus of single layer GS is low, so often considered to be multilayered.

While GSs have been extensively used in many applications of nano-sized devices and systems, the studies of nano-structures using the size-dependent elasticity theories have been an extensive section of research in recent years (Gholami and Ansari 2018, Khetir *et al.* 2017, Akgoz and Civalek 2017, Bounouara *et al.* 2016, Akgoz and Civalek 2017, Akgoz and Civalek 2013, Akgoz and Civalek 2016, Civalek and Demir 2016, Chen and Li 2013, Merkan and Civalek 2016, Akgoz and Civalek 2011, Abdelaziz *et al.* 2017, Meziane *et al.* 2014, Yazid *et al.* 2018, Bellifa *et al.* 2017, Karimi *et al.* 2018, Youcef *et al.* 2018, Ahouel *et al.* 2016, Mokhtar *et al.* 2018, Karimi *et al.* 2018, Chaht *et al.* 2015, Belkorissat *et al.* 2015, Besseghier 2017, Mouffoki *et al.* 2017, Zemri *et al.* 2015, Karimi *et al.* 2017). The functionally graded (FG) plates that the material properties are assumed to vary only in the thickness direction. Many researchers have been investigated the vibration of homogeneous and FG rectangular plates (Akhavan *et al.* 2009, Hosseini-Hashemi *et al.* 2011, Alijani *et al.* 2011, Sobhy 2017, Bellifa *et al.* 2017, El-Haina *et al.* 2017, Bouderba *et al.* 2016, Bousahla *et al.* 2016, Beldielili *et al.*2016, Bellifa *et al.* 2016, Zidi *et al.* 2014, Houari *et al.*2016, Zidi *et al.* 2017). There are many recently researches on beams and plates based on new Quasi-3D shear deformation theory as a new development of advanced structures (Houari *et al.* 2013, Bourada *et al.* 2015, Hebali *et al.* 2014, Bennoun *et al.* 2016, Bousahla *et al.* 2014, Belabed *et al.* 2014, Bouhadra *et al.* 2018, Hamidi *et al.* 2015, Abualnour *et al.* 2018, Younsi *et al.* 2018, Bouafia *et al.* 2017, Benchohra *et al.* 2018, Draiche *et al.* 2016).

The linear and nonlinear equations of motion of GSs using classic plate theory (CLPT) and first order shear deformation plate theory (FSDT) are derived (Bayat *et al.* 2018, Mirzaei *et al.* 2017, Wang *et al.* 1999, Gurses *et al.* 2009, Civalek 2013, Akgoz and Civalek 2011, Gholami *et al.* 2017). Kitipronchai *et al.* (2005) using a continuum model reported the vibration analysis of multi-layered grapheme sheets (MLGS). They derived an explicit formula to predict the van der Waals (vdW) interaction between any two sheets of a MLGS. The mode shapes that are associated

*Corresponding author, Professor
E-mail: Shh@iust.ac.ir

http://www.techno-press.com/journals/sem&subpage=7
ISSN: 1225-4568 (Print), 1598-6217 (Online)

with the natural frequencies are expressed for double layered and ten-layered GSs. The linear and nonlinear vibration analysis of embedded MLGSs under various boundary conditions in the Reissner-Mindlin-type field equation is deal (Wang *et al.* 2015, Jomehzadeh *et al.* 2011).

The classical continuum theory can't describe the size effects. Hence, size dependent continuum theories such as nonlocal elasticity theory, stress-driven nonlocal integral model, nonlocal strain gradient theory and … are developed to consider the small scale effects. The examination of the phenomenon of size effect relevant to nano-structures and carbon nano-tubes has been the focus of several recent models including stress-driven pure and mixture nonlocal integral models. A series of recent contributions on nano-structural modeling employing stress-driven pure and mixture nonlocal integral models can be found in (Barretta *et al.* 2018a-2018g, Apuzzo *et al.* 2017a, Apuzzo *et al.* 2017b, Mahmoudpour *et al.* 2018, Faghidian 2018a-2018c). It is reported that the nonlocal elasticity theory by introducing one length scale parameter is unable to predict the stiffness hardening effects. In the nonlocal strain gradient theory the stress field accounts for not only the nonlocal stress field but also the strain gradients stress field. Mehralian *et al.* (2017a, b) proposed that there is more suitable agreement between the results of nonlocal strain gradient model with MD results in comparison to the nonlocal and strain gradient model. Recently, many researchers have investigated the scaling effects on the mechanical behaviors of nano-beams (Li *et al.* 2016, Khaniki *et al.* 2017) and nanoplates (Ebrahimi *et al.* 2017, Rajabi *et al.* 2017) using nonlocal strain gradient theory.

The Homotopy Analysis Method is a strong and easy-to-use analytic tool for investigating nonlinear problems, which does not need small parameters and suitable not only for weak nonlinear problems, but also for strong nonlinear problems. The most significant feature of this method is it's excellent accuracy for the whole range of oscillation amplitude values. Also, it can be used to solve other conservative truly nonlinear oscillators with complex nonlinearities. The solutions are quickly convergent and its components can be simply calculated. The Homotopy Analysis Method is widely used to investigate the nonlinear vibration behavior of beams and plates. It has been shown that this is a very strong semi-analytical method for highly nonlinear problems (Liao 2012, Kargarnovin *et al.* 2010, Qian *et al.* 2011, Zhao *et al.* 2014, Haghani *et al.* 2018, Mahmoudpour *et al.* 2018, Faghidian 2018b).

He *et al.* (2012) studied the nonlinear forced vibration of MLGSs. They derived a nonlinear explicit expansion for analysis of large amplitude vibration in Taylor expansion of vdW force function. The corresponding amplitude-frequency relationships are investigated. There is a considerable amount of research on the forced vibration analysis of FG nanoplate (Jadhav *et al.* 2013, Wang *et al.* 2017) and homogeneous micro/nano plate (Bayat *et al.* 2017, Shooshtari *et al.* 2017). As the authors know, there isn't any research on nonlinear free and forced vibration of a FG double layered nanoplate (DLNP) embedded in nonlinear medium via nonlocal strain gradient theory.

In the present research, nonlocal strain gradient theory which contains both nonlocal and strain gradient parameters for more accurate description of size effects is employed to investigate the nonlinear free and forced vibration of a Mindlin FG DLNP embedded in a nonlinear elastic medium analytically. The Homotopy Analysis Method is also utilized to solve the nonlinear governing equations of Mindlin FG DLNPs. The parametric study on DLNP dimensions, elastic medium, gradient index would be presented considering the small scale effects on the nonlinear frequency ratios of FG DLNPs. Finally, the frequency-response and phase plane would be discussed.

2. Governing equations

2.1 Nonlocal strain gradient theory

Eringen (1983) showed the nonlocal constitutive behavior of Hookean solids can be represented by the following differential constitutive relation,

$$(1-\mu^2\nabla^2)t_{xx} = E(z)\varepsilon_{xx} \tag{1}$$

Where μ is the nonlocal parameter, t_{xx} is the axial normal stress and ε_{xx} denotes the axial strain. Askes and Aifantis (2011) showed the constitutive relation of the strain gradient theory can be written as,

$$t_{xx} = (1-l^2\nabla^2)E(z)\varepsilon_{xx} \tag{2}$$

Where l is the material characteristic parameter (material length scale parameter). It is recently shown (Li and Hu 2016) the general constitutive relation can be obtained as,

$$(1-\mu^2\nabla^2)t_{xx} = (1-l^2\nabla^2)E(z)\varepsilon_{xx} \tag{3}$$

$$(1-\mu^2\nabla^2)t_{xz} = (1-l^2\nabla^2)G(z)\gamma_{xz} \tag{4}$$

Where $G(z)$ is the shear modulus, t_{xz} stands for shear stress and γ_{xz} denotes the shear strain. Li and Hu (2016) were showed, this particular combination can reasonably explain some nano-size phenomena and there is a good agreement between the results of nonlocal strain gradient theory and the molecular dynamics.

2.2 Single layered nanoplate

An FG single layered nanoplate with length a, width b and thickness h resting on nonlinear elastic foundation under distributed loading is shown in Fig. 1. Since the FG nanoplate is generally composed of two different materials at the top and the bottom surfaces; the elastic modulus $E(z)$ and mass density $\rho(z)$ are assumed to vary in the thickness direction according to the power law distribution (Alijani *et al.* 2011) as,

$$E(z_m) = (E_c - E_m)(\frac{z_m}{h}+\frac{1}{2})^P + E_m \tag{5}$$

$$\rho(z_m) = (\rho_c-\rho_m)\left(\frac{z_m}{h}+\frac{1}{2}\right)^P + \rho_m \tag{6}$$

where the subscripts c and m refer to the ceramic and metal

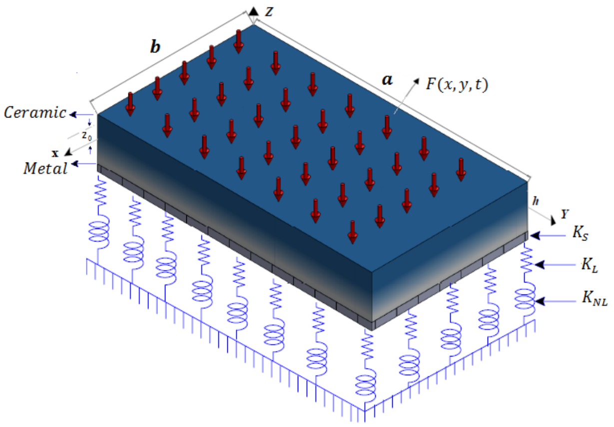

Fig. 1 Geometry of an FG nanoplate resting on nonlinear elastic foundation under distributed loading

phases, respectively, and a gradient index P determines the variation profile of material properties across the FG nanoplate thickness. Poisson's ratio ν is assumed to be constant, i.e., $\nu = 0.3$.

Using the Mindlin plate theory, the displacement field at any point of the nanoplate can be written as

$$u_x(x,y,t) = u(x,y,t) - z\psi_x(x,y,t) \tag{7}$$

$$u_y(x,y,t) = v(x,y,t) - z\psi_y(x,y,t) \tag{8}$$

$$u_z(x,y,t) = w(x,y,t) \tag{9}$$

where u , v and w are the displacement components and ψ_x , ψ_y are the rotational displacements about the y and x axes of the mid-plane at a given point in the nanoplate. In accordance, the von Karman type nonlinear strain-displacement relations may be shown to be (Alijani *et al.* 2011),

$$\varepsilon_{xx} = \frac{\partial u}{\partial x} - z\frac{\partial \psi_x}{\partial x} + \tfrac{1}{2}(\frac{\partial w}{\partial x})^2 \tag{10}$$

$$\varepsilon_{yy} = \frac{\partial v}{\partial y} - z\frac{\partial \psi_y}{\partial y} + \tfrac{1}{2}(\frac{\partial w}{\partial y})^2 \tag{11}$$

$$\varepsilon_{zz} = 0 \tag{12}$$

$$\gamma_{xy} = \frac{\partial u}{\partial y} + \frac{\partial v}{\partial x} + \frac{\partial w}{\partial x}\frac{\partial w}{\partial y} - z(\frac{\partial \psi_x}{\partial y} + \frac{\partial \psi_y}{\partial x}) \tag{13}$$

$$\gamma_{xz} = \frac{\partial w}{\partial x} - \psi_x \tag{14}$$

$$\gamma_{yz} = \frac{\partial w}{\partial y} - \psi_y \tag{15}$$

The stress-strain relations may be expressed as

$$\sigma_{xx} = \frac{E(z)}{1-\nu^2}(\varepsilon_{xx} + \nu\varepsilon_{yy}) \tag{16}$$

$$\sigma_{yy} = \frac{E(z)}{1-\nu^2}(\varepsilon_{yy} + \nu\varepsilon_{xx}) \tag{17}$$

$$\sigma_{zz} = 0 \tag{18}$$

$$\tau_{xy} = G(z)\gamma_{xy} \tag{19}$$

$$\tau_{xz} = G(z)\gamma_{xz} \tag{20}$$

$$\tau_{yz} = G(z)\gamma_{yz} \tag{21}$$

where ν is the Poisson's ratio and G(z) = E(z)/[2(1 + ν)] is the shear modulus. The force and moment resultants relations can be written as

$$M_{ij} = \int_{-\frac{h}{2}}^{\frac{h}{2}} \sigma_{ij} z\, dz\,, \qquad i,j = x,y \tag{22}$$

$$Q_j = \kappa^2 \int_{-\frac{h}{2}}^{\frac{h}{2}} \tau_{jz}\, dz\,, \qquad i,j = x,y \tag{23}$$

Where M_{ij} are the resultant bending and twisting moments and Q_j are the transverse shear forces per unit length. It is noted that the transverse shear force is assumed to be constant in the thickness of nanoplate, therefore, κ^2 is the shear correction factor (Faghidian 2016, 2017).

On the basis of the Mindlin plate theory, the equilibrium equations of motion for nanoplate can be given as follows (Hosseini-Hashemi *et al.* 2011)

$$\frac{\partial N_{xx}}{\partial x} + \frac{\partial N_{xy}}{\partial y} = m_0\frac{\partial^2 u}{\partial t^2} + m_1\frac{\partial^2 \psi_x}{\partial t^2} \tag{24}$$

$$\frac{\partial N_{xy}}{\partial x} + \frac{\partial N_{yy}}{\partial y} = m_0\frac{\partial^2 v}{\partial t^2} + m_1\frac{\partial^2 \psi_y}{\partial t^2} \tag{25}$$

$$\frac{\partial M_{xx}}{\partial x} + \frac{\partial M_{xy}}{\partial y} - Q_x = m_1\frac{\partial^2 u}{\partial t^2} + m_2\frac{\partial^2 \psi_x}{\partial t^2} \tag{26}$$

$$\frac{\partial M_{xy}}{\partial x} + \frac{\partial M_{yy}}{\partial y} - Q_y = m_1\frac{\partial^2 v}{\partial t^2} + m_2\frac{\partial^2 \psi_y}{\partial t^2} \tag{27}$$

$$\begin{aligned}\frac{\partial}{\partial x}\left(N_{xx}\frac{\partial w}{\partial x} + N_{xy}\frac{\partial w}{\partial y}\right) + \frac{\partial}{\partial y}\left(N_{xy}\frac{\partial w}{\partial x} + N_{yy}\frac{\partial w}{\partial y}\right)\\ + \frac{\partial Q_x}{\partial x} + \frac{\partial Q_y}{\partial y} + q = m_0\frac{\partial^2 w}{\partial t^2}\end{aligned} \tag{28}$$

Where m_0, m_1 *and* m_2 are the mass momentum of inertia and are defined as follows

$$\{m_0, m_1, m_2\} = \int_{-\frac{h}{2}-z_0}^{\frac{h}{2}-z_0} \rho(z)\{1, z, z^2\}\, dz\,, \tag{29}$$

Pointed that $z = z_m + z_0$, where z_m is geometric surface and z_0 is physical neutral surface as shown in Fig. 1 and defined as (Li and Yujin 2016),

$$z_0 = \frac{\int_{-\frac{h}{2}}^{\frac{h}{2}} z_m E(z_m) dz_m}{\int_{-\frac{h}{2}}^{\frac{h}{2}} E(z_m) dz_m} \tag{30}$$

Note the first-order mass moment m_1 is neglected, since its contribution is relatively small (Li and Yujin 2016). The transverse loading $F(x,y,t)$ and the surrounding elastic medium interact on lower surface of the nanoplate under consideration as it is shown in Fig. 1. To include the polymer matrix interaction, the nonlinear Pasternak and Winkler foundation models are employed as

$$q = F(x,y,t) - k_w w - k_{NL} w^3 + k_s \nabla^2 w \tag{31}$$

Where k_w, k_s and k_{NL} are the Winkler, Pasternak and nonlinear elastic foundation parameters which depend on the material properties of the polymer matrix. Assuming the harmonic distributed load, $F(x,y,t) = f(t) = f_0\cos(\Omega t)$, is applied on the upper surface of nanoplate and f_0 is the amplitude of the transverse load $F(x,y,t)$ and Ω is the corresponding frequency. In accordance, the nonlocal strain gradient elasticity theory (Eqs. (3) and (4)) and the equations of M_{xx} , M_{yy} and M_{xy} ,the resultant bending and twisting moments, and the transverse shear forces per unit length can be obtained as

$$(1-\mu^2\nabla^2)M_{xx} = -D_1(1-l^2\nabla^2)\left(\frac{\partial\psi_x}{\partial x} + \nu\frac{\partial\psi_y}{\partial y}\right) \tag{32}$$

$$(1-\mu^2\nabla^2)M_{yy} = -D_1(1-l^2\nabla^2)\left(\frac{\partial\psi_y}{\partial y} + \nu\frac{\partial\psi_x}{\partial x}\right) \tag{33}$$

$$\begin{aligned}(1-\mu^2\nabla^2)M_{xy} = -D_1\nu_1(1-l^2\nabla^2)\bigg(&\frac{\partial\psi_x}{\partial y}\\ &+ \nu\frac{\partial\psi_y}{\partial x}\bigg)\end{aligned} \tag{34}$$

$$(1-\mu^2\nabla^2)Q_x = -\kappa^2\nu_1 B_1(1-l^2\nabla^2)\left(\psi_x - \frac{\partial w}{\partial x}\right) \tag{35}$$

$$(1-\mu^2\nabla^2)Q_y = -\kappa^2\nu_1 B_1(1-l^2\nabla^2)\left(\psi_y - \frac{\partial w}{\partial y}\right) \tag{36}$$

Where $\nu_1 = (1-\nu)/2$ .The cross-section parameters are defined as

$$\{B_1, D_1\} = \int_{-\frac{h}{2}-z_0}^{\frac{h}{2}-z_0} \frac{E(z)}{1-\nu^2}\{1, z^2\}dz \tag{37}$$

It is noteworthy that if the axial inertia is neglected, for the nonlinear vibration, Eqs. (24) and (25) will be exactly satisfied by defining the stress function ϕ as follows

$$N_{xx} = \frac{\partial^2\phi}{\partial y^2}\ , \qquad N_{yy} = \frac{\partial^2\phi}{\partial x^2}\ , \qquad N_{xy} = -\frac{\partial^2\phi}{\partial x\partial y} \tag{38}$$

Substituting Eqs. (32)-(36) and Eq. (38) into Eqs. (26)-(28) and doing some algebraic operations would result in the decoupled governing equation of nonlinear forced vibration of thick FG nanoplates in the frameworks of the nonlocal strain gradient elasticity theory as

$$\begin{aligned}&D_1(1-l^2\nabla^2)\nabla^4 w\\ &+ (1-\mu^2\nabla^2)\bigg[m_0\ddot{w}\\ &- \left(m_2 + \frac{D_1 m_0}{\kappa^2\nu_1 B_1}\right)\nabla^2\ddot{w}\bigg]\\ &+ \frac{m_0 m_2}{\kappa^2\nu_1 B_1}(1-\mu^2\nabla^2)^2\ddddot{w}\\ &= (1-\mu^2\nabla^2)(f^* + N^*)\end{aligned} \tag{39}$$

where the dot denotes the d/dt and

$$N^* = \left[N - \frac{D_1}{\kappa^2\nu_1 B_1}\nabla^2 N\right] + \frac{m_2}{\kappa^2\nu_1 B_1}(1-\mu^2\nabla^2)\ddot{N} \tag{40a}$$

$$f^* = \left[q - \frac{D_1}{\kappa^2\nu_1 B_1}\nabla^2 q\right] + \frac{m_2}{\kappa^2\nu_1 B_1}(1-\mu^2\nabla^2)\ddot{q} \tag{40b}$$

where, N is defined as (Wang *et al.* 2015)

$$N = \frac{\partial^2\phi}{\partial y^2}\frac{\partial^2 w}{\partial x^2} + \frac{\partial^2\phi}{\partial x^2}\frac{\partial^2 w}{\partial y^2} - 2\frac{\partial^2\phi}{\partial x\partial y}\frac{\partial^2 w}{\partial x\partial y} \tag{41}$$

Eq. (41) is in terms of stress function and transverse displacement and it must to be augmented with a compatibility equation. The compatibility equation can be obtained by expressing the in-plane strain components in terms of stress function as

$$\begin{aligned}\nabla^4\phi &= A_1\left[\left(\frac{\partial^2 w}{\partial x\partial y}\right)^2 - \frac{\partial^2 w}{\partial x^2}\frac{\partial^2 w}{\partial y^2}\right]\ ,\\ A_1 &= \int_{-\frac{h}{2}-z_0}^{\frac{h}{2}-z_0} E(z)dz\end{aligned} \tag{42}$$

All edges are considered simply supported boundary condition with movable in-plane edges, thus the general solution for stress function ϕ can be obtained as

$$\begin{aligned}\phi(x,y) = \frac{A_1}{32n^2m^2a^2b^2}\bigg[&m^4a^4cos\left(\frac{2n\pi x}{a}\right)\\ &+ n^4b^4cos\left(\frac{2m\pi y}{b}\right)\bigg]q(t)^2\end{aligned} \tag{43}$$

The classical and non-classical boundary condition need to be considered in the case of nonlocal strain gradient plates with simply supported as follow (Rajabi *et al.* 2017)

$$\begin{aligned}&classical: && w = 0\,, M_{xx} = 0 \quad at\ edges\ x = 0, a\\ &classical: && w = 0\,, M_{yy} = 0 \quad at\ edges\ y = 0, b\\ &non-classical: && M_{xxx}^{(1)} = 0, Q_{xzx}^{(1)} = 0 \quad at\ edges\ x = 0, a\\ &non-classical: && M_{xxy}^{(1)} = 0, Q_{xzy}^{(1)} = 0 \quad at\ edges\ y = 0, b\end{aligned} \tag{44}$$

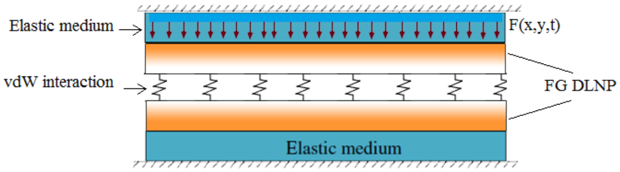

Fig. 2 A side view of an FG DLNP embedded in an elastic matrix under distributed loading

2.3 Double layered nanoplate

An FG DLNP embedded in an elastic medium under uniform distributed loading on upper layer is shown in Fig. 2.

The van der Waals (vdW) interaction between the layers of FG DLNP is modeled as Winkler foundation (Wang *et al.* 2015). Therefore, the vdW forces acting on layers of DLNP can be written as

$$q_1 = -c(w_1 - w_2) \;, \qquad q_2 = -c(w_2 - w_1) \tag{45}$$

Where c is the vdW interaction coefficient. According to Eqs. (39) and (43) the governing equations of nonlinear forced vibration of thick FG DLNP based on nonlocal strain gradient theory can be derived as

$$\begin{aligned} &D_1(1-l^2\nabla^2)\nabla^4 w_1 \\ &+(1-\mu^2\nabla^2)\left[m_0\ddot{w}_1 - \left(m_2+\frac{D_1 m_0}{\kappa^2 \nu_1 B_1}\right)\nabla^2\ddot{w}_1\right] \\ &+\frac{m_0 m_2}{\kappa^2 \nu_1 B_1}(1-\mu^2\nabla^2)^2 \ddddot{w}_1 \\ &=(1-\mu^2\nabla^2)(f_1^* + N_1^* - C_1^*) \end{aligned} \tag{46}$$

$$\nabla^4\phi_1 = A_1\left[\left(\frac{\partial^2 w_1}{\partial x\partial y}\right)^2 - \frac{\partial^2 w_1}{\partial x^2}\frac{\partial^2 w_1}{\partial y^2}\right] \tag{47}$$

$$\begin{aligned} &D_1(1-l^2\nabla^2)\nabla^4 w_2 \\ &+(1-\mu^2\nabla^2)\left[m_0\ddot{w}_2 - \left(m_2+\frac{D_1 m_0}{\kappa^2 \nu_1 B_1}\right)\nabla^2\ddot{w}_2\right] \\ &+\frac{m_0 m_2}{\kappa^2 \nu_1 B_1}(1-\mu^2\nabla^2)^2 \ddddot{w}_2 \\ &=(1-\mu^2\nabla^2)(f_2^* + N_2^* - C_2^*) \end{aligned} \tag{48}$$

$$\nabla^4\phi_2 = A_1\left[\left(\frac{\partial^2 w_2}{\partial x\partial y}\right)^2 - \frac{\partial^2 w_2}{\partial x^2}\frac{\partial^2 w_2}{\partial y^2}\right] \tag{49}$$

Where $f_1^*, N_1^*, C_1^*, f_2^*, N_2^*, C_2^*$ are listed in the appendix, equation (A.1). The subscript 1 and 2 for the variables are used to indicate the upper and lower layers of FG DLNP, respectively. Furthermore, to reduce the nonlinear partial differential equations of nonlinear forced vibration of FG DLNP based on nonlocal strain gradient theory Eqs. (46) and (48) into a time-varying set of ordinary differential equations, the Galerkin method would be employed here. To this end, the displacement function is supposed to have the separable form of,

$$w_i = \sum_{m=1}^{\infty}\sum_{n=1}^{\infty} W_{imn}(t)\psi_{imn}(x,y) \;, \qquad i = 1,2 \tag{50}$$

where $W_{imn}(t)$ is a time base-function to be determined later and $\psi_{imn}(x,y)$ is the linear spatial mode shape. Considering the simply supported boundary conditions, an appropriate approximation for mode shape $\varphi_{imn}(x,y)$ can be expressed as (Wang *et al.* 2015),

$$\psi_{imn}(x,y) = \sum_{m=1}^{\infty}\sum_{n=1}^{\infty} \sin\left(\frac{m\pi x}{a}\right)\sin\left(\frac{n\pi y}{b}\right) \;, i = 1,2 \tag{51}$$

The governing equation of the time base-function in nonlinear forced vibration of FG DLNP based on nonlocal strain gradient theory could be determined substituting Eq. (50) into Eqs. (46) and (48) and subsequently multiplying by the linear spatial mode shape and finally integrating along the nanoplate's dimensions as,

$$\begin{aligned} &\begin{bmatrix}\ddddot{W}_1\\ \ddddot{W}_2\end{bmatrix} + \begin{bmatrix}\alpha_1 & \alpha_6\\ \alpha_6 & \alpha_1\end{bmatrix}\begin{bmatrix}\ddot{W}_1\\ \ddot{W}_2\end{bmatrix} + \begin{bmatrix}\alpha_3 & \alpha_7\\ \alpha_7 & \alpha_3\end{bmatrix}\begin{bmatrix}W_1\\ W_2\end{bmatrix} \\ &+\begin{bmatrix}\alpha_2 & 0\\ 0 & \alpha_2\end{bmatrix}\begin{bmatrix}W_1^2\ddot{W}_1\\ W_2^2\ddot{W}_2\end{bmatrix} \\ &+\begin{bmatrix}\alpha_4 & 0\\ 0 & \alpha_4\end{bmatrix}\begin{bmatrix}W_1\dot{W}_1^2\\ W_2\dot{W}_2^2\end{bmatrix} \\ &+\begin{bmatrix}\alpha_5 & 0\\ 0 & \alpha_5\end{bmatrix}\begin{bmatrix}W_1^3\\ W_2^3\end{bmatrix} \\ &=\begin{bmatrix}\alpha_8\\ 0\end{bmatrix}f(t) + \begin{bmatrix}\alpha_9\\ 0\end{bmatrix}\ddot{f}(t) \end{aligned} \tag{52}$$

Where $\alpha's$ are introduced as,

$$\alpha_1 = \frac{a^2b^2\left(m_0 + m_2(c+k_l)\hat{G}\right) + (a^2+b^2)\pi^2\left(m_0(\hat{G}D_1+\mu^2) + k_s m_2\hat{G} + m_2 + m_2\mu^2(c+k_l+\hat{A}k_s)\hat{G}\right)}{m_0 m_2\hat{G}[a^2b^2 + (a^2+b^2)\pi^2\mu^2]} \tag{53}$$

$$\alpha_2 = \frac{3[A_1(a^4+b^4)\pi^4 + 9a^4b^4k_{NL}]}{16a^4b^4m_0} \tag{54}$$

$$+\frac{\hat{A}^2a^4b^4\left[k_s\mu^2 + D_1\left(1+\hat{G}(k_s+(c+k_l)\mu^2)\right) + \hat{A}D_1(\hat{G}k_s\mu^2 + l^2)\right]}{m_0 m_2\hat{G}[a^2b^2+(a^2+b^2)\pi^2\mu^2]^2} \tag{55}$$

$$\alpha_4 = \frac{6[A_1(a^4+b^4)\pi^4 + 9a^4b^4k_{NL}]}{16a^4b^4m_0} \tag{56}$$

$$\alpha_5 = \frac{[A_1(a^4+b^4)\pi^4 + 9a^4b^4k_{NL}][a^2b^2 + (a^2+b^2)\pi^2(\hat{G}D_1+\mu^2)]}{16a^4b^4m_0m_2\hat{G}[a^2\underset{c}{b^2} + (a^2+b^2)\pi^2\mu^2]} \tag{57}$$

$$\alpha_6 = -\frac{c}{m_0} \tag{58}$$

$$\alpha_7 = -\frac{c[a^2b^2 + (a^2+b^2)\pi^2(\hat{G}D_1+\mu^2)]}{m_0m_2\hat{G}[a^2b^2+(a^2+b^2)\pi^2\mu^2]} \tag{59}$$

$$\alpha_8 = \frac{\left[a^2b^2 + (a^2+b^2)\pi^2\hat{G}D\right]}{m_0 m_2 \hat{G}[a^2b^2 + (a^2+b^2)\pi^2\mu^2]} \tag{60}$$

$$\alpha_9 = \frac{1}{m_0} \tag{61}$$

That $\hat{G}$ and $\hat{A}$ are defined as

$$\hat{G} = \frac{1}{\kappa^2 \nu_1 B_1} \quad , \quad \hat{A} = \frac{(a^2+b^2)\pi^2}{a^2b^2} \tag{62}$$

By neglecting the transvers shear deformation and rotary inertia the classical nonlinear forced vibration of FG DLNP is obtained, as follows

$$\begin{bmatrix}\alpha_1^* & 0\\ 0 & \alpha_1^*\end{bmatrix}\begin{bmatrix}\ddot{W}_1\\ \ddot{W}_2\end{bmatrix} + \begin{bmatrix}\alpha_2^* & \alpha_4^*\\ \alpha_4^* & \alpha_2^*\end{bmatrix}\begin{bmatrix}W_1\\ W_2\end{bmatrix} + \begin{bmatrix}\alpha_3^* & 0\\ 0 & \alpha_3^*\end{bmatrix}\begin{bmatrix}W_1^3\\ W_2^3\end{bmatrix} = \begin{bmatrix}\alpha_5^*\\ 0\end{bmatrix} f(t) \tag{63}$$

Where $\alpha^{*\prime}s$ are introduced as,

$$\alpha_1^* = 16a^4b^4m_0[a^2b^2 + (a^2+b^2)\pi^2\mu^2] \tag{64}$$

$$\alpha_2^* = 16a^2b^2\left[a^4b^4c + \hat{A}^3\,\pi^6a^4b^4D_1l^2 + ca^2b^2(a^2+b^2)\pi^2\mu^2\right] \tag{65}$$

$$\alpha_3^* = A_1\pi^2(a^4+b^4)[a^2b^2 + (a^2+b^2)\pi^2\mu^2] \tag{66}$$

$$\alpha_4^* = -16a^4b^4c[a^2b^2 + (a^2+b^2)\pi^2\mu^2] \tag{67}$$

$$\alpha_5^* = 16a^6b^6[a^2b^2 + (a^2+b^2)\pi^2\mu^2] \tag{68}$$

In order to decoupling the Eq. (52), the coordinate transformation $\boldsymbol{W} = \boldsymbol{Xq}$ is defined. Where $\boldsymbol{q} = [q_1, q_2]^T$ and the transition matrix $\boldsymbol{X}$ can be chosen as $\boldsymbol{X} = \begin{bmatrix}1 & 1\\ 1 & -1\end{bmatrix}$. Then the nonlinear decoupled equations of FG DLNP can be rewritten as

$$\begin{bmatrix}\ddot{\ddot{q}}_1\\ \ddot{\ddot{q}}_2\end{bmatrix} + \begin{bmatrix}\alpha_1+\alpha_6 & 0\\ 0 & \alpha_1-\alpha_6\end{bmatrix}\begin{bmatrix}\ddot{q}_1\\ \ddot{q}_2\end{bmatrix} + \begin{bmatrix}\alpha_3+\alpha_7 & 0\\ 0 & \alpha_3-\alpha_7\end{bmatrix}\begin{bmatrix}q_1\\ q_2\end{bmatrix} + \begin{bmatrix}\alpha_2 & 0\\ 0 & \alpha_2\end{bmatrix}\begin{bmatrix}q_1^2\ddot{q}_1\\ q_2^2\ddot{q}_2\end{bmatrix} + \begin{bmatrix}\alpha_4 & 0\\ 0 & \alpha_4\end{bmatrix}\begin{bmatrix}q_1\dot{q}_1^2\\ q_2\dot{q}_2^2\end{bmatrix} + \begin{bmatrix}\alpha_5 & 0\\ 0 & \alpha_5\end{bmatrix}\begin{bmatrix}q_1^3\\ q_2^3\end{bmatrix} = \frac{1}{2}\begin{bmatrix}\alpha_8\\ \alpha_8\end{bmatrix} f(t) + \frac{1}{2}\begin{bmatrix}\alpha_9\\ \alpha_9\end{bmatrix}\ddot{f}(t) \tag{69}$$

$f(t)$ is assumed to applied orthogonally on the first layer of FG DLNP (Fig. 1), with harmonic excitation $f(t) = f_0\cos(\Omega t)$, where f_0 is force magnitude, t is the time and Ω is the excitation frequency.

3. Free vibration analysis

The governing equations for nonlinear free vibration analysis can be obtained setting $f(t) = 0$. Also, if the nonlinear terms eliminating in the Eq. (69), the linear form of governing equations is achieved as

$$\begin{bmatrix}\ddot{\ddot{q}}_1\\ \ddot{\ddot{q}}_2\end{bmatrix} + \begin{bmatrix}\alpha_1+\alpha_6 & 0\\ 0 & \alpha_1-\alpha_6\end{bmatrix}\begin{bmatrix}\ddot{q}_1\\ \ddot{q}_2\end{bmatrix} + \begin{bmatrix}\alpha_3+\alpha_7 & 0\\ 0 & \alpha_3-\alpha_7\end{bmatrix}\begin{bmatrix}q_1\\ q_2\end{bmatrix} = \begin{bmatrix}0\\ 0\end{bmatrix} \tag{70}$$

From Eq. (70) the linear natural frequencies can be obtained as

$$\omega_{L1} = \sqrt{\frac{(\alpha_1+\alpha_6) - \sqrt{(\alpha_1+\alpha_6)^2 - 4(\alpha_3+\alpha_7)}}{2}} \tag{71}$$

$$\omega_{L2} = \sqrt{\frac{(\alpha_1-\alpha_6) - \sqrt{(\alpha_1-\alpha_6)^2 - 4(\alpha_3-\alpha_7)}}{2}} \tag{72}$$

The decoupled nonlinear equation for $q_1(t)$ is as

$$\ddot{\ddot{q}}_1(t) + (\alpha_1+\alpha_6)\ddot{q}_1(t) + (\alpha_3+\alpha_7)q_1(t) + \alpha_2q_1^2\ddot{q}_1(t) + \alpha_4q_1\dot{q}_1^2 + \alpha_5q_1^3(t) = 0 \tag{73}$$

The initial conditions for Eq. (73) would be assumed to be,

$$\begin{cases} q_1(0) = a_0\\ \dot{q}_1(0) = 0\\ \ddot{q}_1(0) = 0\\ \dddot{q}_1(0) = 0 \end{cases} \tag{74}$$

where a_0 is maximum amplitude corresponding to the time base-function $q_1(t)$. To solve the Eq. (73) the homotopy analysis method is employed that would be introduced.

4. Solution method

4.1 Homotopy Analysis Method

Homotopy Analysis Method (HAM) is a general analytic method for solving the non-linear differential equations that successfully result in convergent series solutions of strongly nonlinear problems. The HAM transforms a non-linear differential equation into infinite numbers of linear differential equations with embedding an auxiliary parameter p that typically ranges from zero to one. As p increases from 0 to 1, the solution varies from the initial guess to the exact solution (Liao 2012). To illustrate the basic ideas of the HAM, consider the following nonlinear differential equation

$$\mathcal{N}[q(t)] = 0 \tag{75}$$

where $\mathcal{N}$ is a nonlinear operator and t denotes time as the independent variable and $q\ (t)$ is an unknown function to be determined. The homotopy function is constructed as follows (Liao 2012)

$$\bar{H}(\varphi;p,\hbar,H(t))=(1-p)\mathcal{L}[\varphi(t;p)-q_0(t)] \\ -p\hbar H(t)\mathcal{N}[\varphi(t;p)] \tag{76}$$

Where φ is a function of t and p and also ħ and $H(t)$ are non-zero auxiliary parameter and non-zero auxiliary function, respectively. The parameter $\mathcal{L}$ denotes an auxiliary linear operator. As p increases from 0 to 1, $\varphi(t;p)$ varies from the initial approximation to the exact solution. So, the zero-order deformation is constructed as (Liao 2012),

$$(1-p)\mathcal{L}[\varphi(t;p)-q_0(t)]=p\hbar H(t)\mathcal{N}[\varphi(t;p)] \tag{77}$$

with the following initial conditions corresponding to initial conditions of Eq. (73),

$$\varphi(0;p)=a_0 \quad , \quad \frac{d\varphi(0;p)}{dt}=0 \tag{78}$$

The higher order approximations of the solution can be obtained by calculating the m-order (m>1) deformation equation as (Liao 2012),

$$\mathcal{L}[q_m-\chi q_{m-1}]=\hbar H(t)R_m(q_{m-1},\omega_{m-1}) \tag{79}$$

where the χ and $R_m(q_{m-1},\omega_{m-1})$ are defined as follows (Liao 2012),

$$R_m(q_{m-1},\omega_{m-1}) \\ =\frac{1}{(m-1)!}\frac{\partial^{m-1}\mathcal{N}[\varphi(t;p),\omega(p)]}{\partial p^{m-1}}|p=0 \tag{80}$$

$$\chi=\begin{cases}0 & m\le 1\\ 1 & m\ge 2\end{cases} \tag{81}$$

Subjected to the following homogeneous initial conditions, since the initial conditions of Eq. (73) are already imposed to the zero-order deformation,

$$q_m(0)=\dot{q_m}(0)=\ddot{q}_m(0)=\dddot{q}_m(0)=0 \tag{82}$$

4.2 Application of the HAM

The decoupled governing equation for nonlinear free vibration of FG DLNP in elastic medium based on nonlocal strain gradient theory is obtained as,

$$\ddddot{q}_1(t)+\beta_1\ddot{q}_1(t)+\beta_2 q_1(t)+\beta_3 q_1^2\ddot{q}_1(t)+\beta_4 q_1\dot{q}_1^2 \\ +\beta_5 q_1^3(t)=0 \tag{83}$$

where $\beta_1=\alpha_1+\alpha_6$, $\beta_2=\alpha_3+\alpha_7$, $\beta_3=\alpha_2$, $\beta_4=\alpha_4$ and $\beta_5=\alpha_5$. In order to solve the Eq. (83) through HAM, the first conjecture of the problem solution, which satisfies initial conditions Eq. (82), can be stated as follows,

$$q_{10}(t)=A\cos(\omega_1 t)+Bcos(\omega_2 t) \tag{84}$$

$$q_{10}(0)=a_0\,,\dot{q}_{10}(0)=\ddot{q}_{10}(0)=\dddot{q}_{10}(0)=0 \tag{85}$$

Where a_0 is the maximum amplitude of vibration and ω_1 and ω_2 are the first and the second nonlinear frequency of FG DLNP, respectively. According to initial condition the A and B coefficients are obtained as,

Table 1 Linear natural frequency of DLNP (THz)

Frequency	Bending mode		Shear mode
	Present (FSDT)	Jomehzadeh *et al.* (2011) (CLPT)	Present (FSDT)
ω_{L1}	0.0663	0.0667	20.7678
ω_{L2}	2.6726	2.6807	

$$A=-\frac{a_0{\omega_2}^2}{{\omega_1}^2-{\omega_2}^2} \quad , \quad B=\frac{a_0{\omega_1}^2}{{\omega_1}^2-{\omega_2}^2} \tag{86}$$

According to Liao (2012) the auxiliary linear operator can be expressed in a general form

$$\mathcal{L}(u)=\left[\prod_{i=1}^{k}\left(\frac{d^2}{dt^2}+\omega_i^2\right)\right]u \tag{87}$$

Thus for $k=2$ the auxiliary linear operator and nonlinear operator are as follows,

$$\mathcal{L}[q_{11}(t,p)]=\ddddot{q}_{11}(t,p)+({\omega_1}^2+{\omega_2}^2)\ddot{q}_{11}(t,p) \\ +(\omega_1\omega_2)^2 q_{11}(t,p) \tag{88}$$

$$\mathcal{N}[q_{11}(t,p)]=\ddddot{q}_{11}(t)+\beta_1\ddot{q}_{11}(t)+\beta_2 q_{11}(t) \\ +\beta_3 q_{11}^2\ddot{q}_{11}(t)+\beta_4 q_{11}\dot{q}_{11}^2 \\ +\beta_5 q_{11}^3(t) \tag{89}$$

The first-order deformation equation which gives the first-order approximation of the $q_{11}(t)$ can be written as

$$\mathcal{L}[q_{11}(t)]=\hbar H(t)\mathcal{N}[q_{11}(t,p),\omega]_{p=0} \tag{90}$$

$$q_{11}(0)=\dot{q}_{11}(0)=\ddot{q}_{11}(0)=\dddot{q}_{11}(0)=0 \tag{91}$$

The auxiliary function $H(t)$ and the auxiliary parameter ħ which adjust convergence region and rate of approximate solution must be chosen in such a way that the solution of Eq. (79) could be expressed by a set of base-functions. While assuming ħ = -1 and $H(\tau)=1$ can satisfy this constraint (Liao 2012), as a result the first-order deformation equation of Eq. (79) utilizing the $q_0(t)$as Eq. (84) may be shown to be,

$$\ddddot{q}_{11}(t,p)+({\omega_1}^2+{\omega_2}^2)\ddot{q}_{11}(t,p) \\ +(\omega_1\omega_2)^2 q_{11}(t,p) \\ =E_1cos(\omega_1 t)+E_2cos(\omega_2 t) \\ +E_3cos(3\omega_1 t)+E_4cos(3\omega_2 t) \\ +E_5cos(\omega_1-2\omega_2)t \\ +E_6cos(2\omega_1-\omega_2)t \\ +E_7cos(\omega_1+2\omega_2)t \\ +E_8cos(2\omega_1+\omega_2)t \tag{92}$$

where E’s are given in the Appendix, Eq. (A.2). To prevent so-called secular terms in the time response, the coefficients of the terms $\cos(\omega_1 t)$ and $\cos(\omega_2 t)$ are set to zero and consequently, two algebraic equations which yield the nonlinear natural frequencies of FG DLNP would be achieved as,

$$\omega_1^8 - \left(2\omega_2^2 + \beta_1 + \tfrac{1}{2}\beta_3 a_0^2\right)\omega_1^6 + \left(\omega_2^4 + \left(2\beta_1 - \beta_3 a_0^2 + \tfrac{1}{2}\beta_4 a_0^2\right)\omega_2^2 + \beta_2 + \tfrac{3}{2}\beta_5 a_0^2\right)\omega_1^4 - \left(\left(\beta_1 + \tfrac{3}{4}\beta_3 a_0^2 - \tfrac{1}{4}\beta_4 a_0^2\right)\omega_2^4 + 2\beta_2\omega_2^2\right)\omega_1^2 + \tfrac{3}{4}\beta_5 a_0^2\omega_2^4 + \beta_2\omega_2^4 = 0 \tag{93}$$

$$\omega_2^8 - \left(2\omega_1^2 + \beta_1 + \tfrac{1}{2}\beta_3 a_0^2\right)\omega_2^6 + \left(\omega_1^4 + \left(2\beta_1 - \beta_3 a_0^2 + \tfrac{1}{2}\beta_4 a_0^2\right)\omega_1^2 + \beta_2 + \tfrac{3}{2}\beta_5 a_0^2\right)\omega_2^4 - \left(\left(\beta_1 + \tfrac{3}{4}\beta_3 a_0^2 - \tfrac{1}{4}\beta_4 a_0^2\right)\omega_1^4 + 2\beta_2\omega_1^2\right)\omega_2^2 + \tfrac{3}{4}\beta_5 a_0^2\omega_1^4 + \beta_2\omega_1^4 = 0 \tag{94}$$

Solving Eq. (92), the $q_{11}(t)$ is obtained as follows

$$q_{11}(t) = H_1 cos(\omega_1 t) + H_2 cos(\omega_2 t) + H_3 cos(3\omega_1 t) + H_4 cos(3\omega_2 t) + H_5 cos(\omega_1 - 2\omega_2)t + H_6 cos(2\omega_1 - \omega_2)t + H_7 cos(\omega_1 + 2\omega_2)t + H_8 cos(2\omega_1 + \omega_2)t \tag{95}$$

Where H_1 and H_2 are obtained by applying initial conditions. Coefficients H's have been presented in the appendix, equation (A.3). Finally, the first-order approximation of the $q_1(t)$ presented as

$$q_1(t) = q_{10}(t) + q_{11}(t) \tag{96}$$

If the above steps done for $q_2(t)$, the first-order approximation of the nonlinear natural frequency for FG DLNP would be obtained. It is interesting in to note that the zero-order approximation of the nonlinear natural frequencies of FG DLNP embedded in elastic matrix based on nonlocal strain gradient elasticity theory can be obtained from Eqs. (93) and (94).

4.3 Nonlinear forced vibration

Substituting harmonic excitation force into Eq. (83), the nonlinear forced vibration of the first layer is achieved

$$\ddot{q}_1 + \beta_1\ddot{q}_1 + \beta_2 q_1 + \beta_3 q_1^2\ddot{q}_1 + \beta_4 q_1\dot{q}_1^2 + \beta_5 q_1^3 = \beta_6 f_0 \cos(\Omega t) \tag{97}$$

where $\beta_6 = 0.5 * (\alpha_8 - \Omega^2\alpha_9)$. According to Harmonic Balanced method (HB), the particular solution of Eq. (97) is assumed

$$q_1(t) = A_1\cos(\Omega t) + A_2\sin(\Omega t) \quad , \quad A^2 = A_1^2 + A_2^2 \tag{98}$$

where A denotes the amplitude of the forced vibration. The value of A can be determined by substituting Eq. (98) into Eq. (97), which yields

$$\Omega^4(A_1\cos(\Omega t) + A_2\sin(\Omega t)) - \beta_1\Omega^2(A_1\cos(\Omega t) + A_2\sin(\Omega t)) + \beta_2(A_1\cos(\Omega t) + A_2\sin(\Omega t)) - \beta_3\Omega^2(A_1\cos(\Omega t) + A_2\sin(\Omega t))^2(A_1\cos(\Omega t) + A_2\sin(\Omega t)) + \beta_4\Omega^2(A_1\cos(\Omega t) + A_2\sin(\Omega t))(-A_1\sin(\Omega t) + A_2\cos(\Omega t))^2 + \beta_5(A_1\cos(\Omega t) + A_2\sin(\Omega t))^3 = \beta_6 f_0\cos(\Omega t) \tag{99}$$

with the use of the trigonometric relations, the Eq. (99) simplifies as follows

$$A_1\left(\beta_2 + \frac{3}{4}A^2\beta_5 - \beta_1\Omega^2 - \frac{3}{4}A^2\Omega^2\beta_3 + \frac{1}{4}A^2\Omega^2\beta_4 + \Omega^4\right)\cos(\Omega t) + A_2\left(\beta_2 + \frac{3}{4}A^2\beta_5 - \beta_1\Omega^2 - \frac{3}{4}A^2\Omega^2\beta_3 + \frac{1}{4}A^2\Omega^2\beta_4 + \Omega^4\right)\sin(\Omega t) = \beta_6 f_0\cos(\Omega t) \tag{100}$$

Equating the coefficients of $\cos(\Omega t)$ and $\sin(\Omega t)$ on both sides of the resulting equation and doing some mathematical manipulation the amplitude-frequency relation is achieved

$$A^2\left(\Omega^4 - \beta_1\Omega^2 + \beta_2 + \frac{1}{4}(\Omega^2\beta_4 - 3\Omega^2\beta_3 + 3\beta_5)A^2\right)^2 - (\beta_6 f_0)^2 = 0 \tag{101}$$

5. Result and discussion

A comparative study for evaluation of linear natural

Table 2 Comparison of the dimensionless linear frequencies $\varpi = \omega h\sqrt{\rho_c/E_c}$ of FG square plate (Al/Al_2O_3)

$\frac{h}{a}$	*Sources*	*Power Law Index (P)* 0	1	4	10	∞
0.05	Present	0.0148	0.0102	0.0092	0.0085	0.0075
	Hosseini-Hashemi *et al.* 2011	0.0148	0.0113	0.0098	0.0094	-
0.1	Present	0.0577	0.0400	0.0357	0.0330	0.0293
	Hosseini-Hashemi *et al.* 2011	0.0577	0.0442	0.0382	0.0366	0.0293

Table 3 Material properties of FG nanoplate (Alijani *et al.* 2011)

Material	Young's modulus	Poisson's ratio	Mass density	Thermal expansion coefficient
	(GPa)		(kg/m^3)	$1/K^{\circ}$
SUS304	207.8	0.3	8166	12.33×10^{-6}
Si_3N_4	322.3	0.3	2370	5.87×10^{-6}

Table 4 Comparison of nonlinear to linear frequency ratio ω_{NL}/ω_L of FGM square plate ($P = 2$)

solution method	a_0/h 0.0	0.2	0.4	0.6	0.8	1.0
Perturbation (Huang and Shen 2004*)*	1.000	1.021	1.081	1.174	1.293	1.432
HAM (Present)	1.000	1.021	1.083	1.178	1.300	1.442

frequencies of double layered nanoplate with those obtained by Jomehzadeh *et al.* (2011) is carried out in Table 1 for simply supported isotropic DLNP with $a = 10\,nm$, $b = 10\,nm$, $h = 0.34\,nm$, $E = 1.02\,TPa$, $\nu = 0.16$ and $\rho = 2250\ kg/m^3$.

It is observed that the present results agree well with those given by (Jomehzadeh *et al.* 2011). It is noteworthy that the present results are less than Jomehzadeh *et al.* (2011) because the CLPT overestimates the vibration frequencies due to the neglecting transverse shear deformation and rotary inertia of nanoplates. It is found from Table 1 that the second frequency of bending mode is greater than the first frequency, and this is due to the vdW coefficient. Also, the frequency obtained from the shear mode is much greater than bending mode, and the classical plate theory dose not form the sheet of this mode because it neglects the transverse shear deformation. In Table 2, the dimensionless natural frequencies of the simply supported square FG plates for two values of the thickness to length ratios are presented. It is seen that the present results are reported the good agreement with exact solution that those obtained by (Hosseini-Hashemi *et al.* 2011).

An FG nanoplate is considered as a case study to illustrate the general behavior of functionally graded nanoplates when the gradient index is set to be $P = 1$, the dimensions of nanoplate are $a = 10\,nm$, $b = 10\,nm$, $h = 1\,nm$, $c = 108\times 10^{18}$, $\kappa^2 = 5/6$. The nanoplate is assumed to be made of $Si_3N_4 - SUS304$ whose material

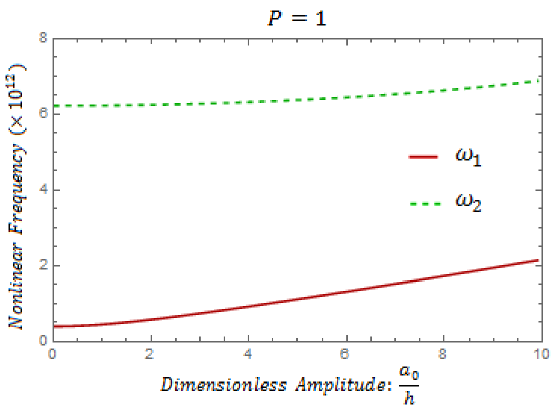

Fig. 3 Nonlinear frequencies versus dimensionless amplitude. ($a/b = 1, h/a = 0.1, \mu = 0.1\,nm, l = 1\,nm$)

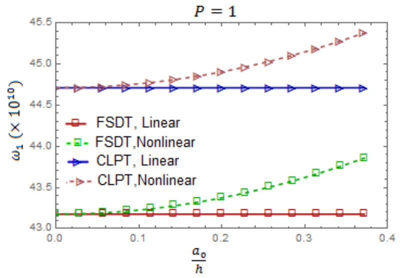

(a) $\frac{b}{h} = 10$

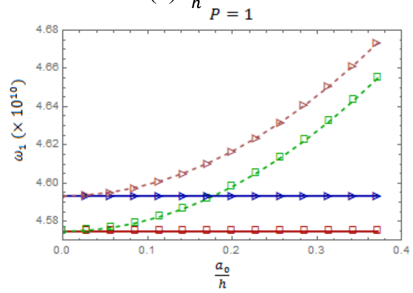

(b) $\frac{b}{h} = 30$

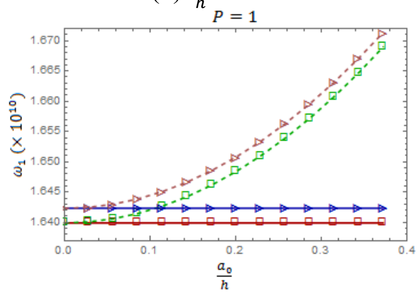

(c) $\frac{b}{h} = 50$

Fig. 4 First linear and nonlinear frequency versus dimensionless amplitude of an FG DLNP for different length-thickness ratio. ($\mu = 0.1\,nm$, $l = 1\,nm$)

properties are listed in Table 3.

In order to evaluation of HAM results the nonlinear to linear frequency ratio is calculated and compared in Table 4 with the results of Huang and Shen (2004) based on the perturbation technique.

Table 4 shows that the present results agree well with perturbation results.

The variation of the nonlinear bending frequencies of

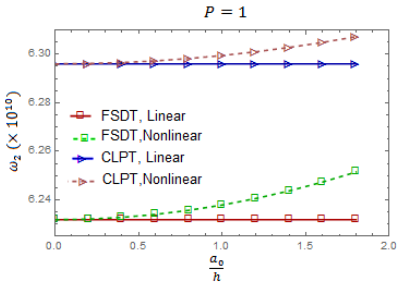

(a) $\frac{b}{h} = 10$

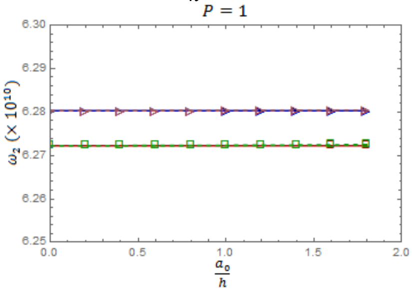

(b) $\frac{b}{h} = 30$

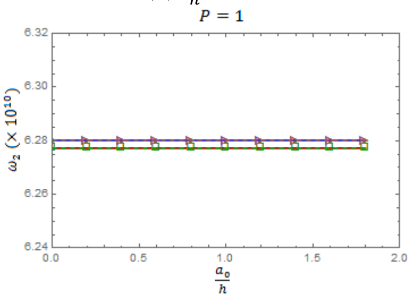

(c) $\frac{b}{h} = 50$

Fig. 5 Second linear and nonlinear frequency versus dimensionless amplitude of an FG DLNP for different length-thickness ratio. ($\mu = 0.1\ nm\ , l = 1\ nm$)

DLNP versus dimensionless amplitude is shown in Fig. 3. It can be seen that the nonlinear frequencies get larger with increasing dimensionless amplitude. This effect is attributed to the intrinsic stiffening effect brought by geometric nonlinearity of the FG DLNP. In the region $a_0/h < 10$ as it is seen from Fig. 3, the ω_{NL1} represents a linear variation whereas the ω_{NL2} variation remains almost unchanged and this is due to the vdW coefficient.

In order to investigate the significances of length-thickness ratio and geometric nonlinearity on the mechanical behavior of FG DLNP, the vibration frequencies are compared. Fig. 4 shows that the nonlinear frequencies are generally higher than linear frequencies for the same amplitude. Also, it can be seen the differences between the FSDT and CLPT. As expected, the CLPT overestimates the linear and nonlinear frequencies due to the neglecting transverse shear deformation and rotary inertia of FG nanoplates. Furthermore, when considering a small length – thickness ratio, the effect of the transverse shear deformation is significant.

Fig. 5 shows that the second linear and nonlinear frequency has the same behavior as the first frequency, except that when $b/h > 20$ the effect of dimensionless amplitude on the vibration frequencies is very low.

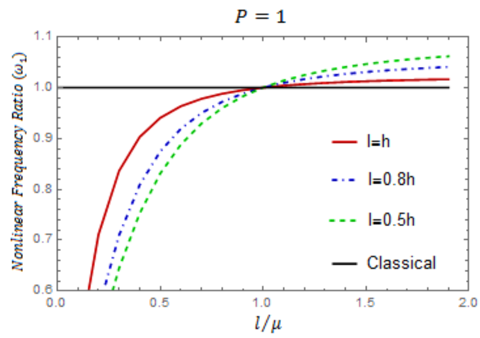

(a)

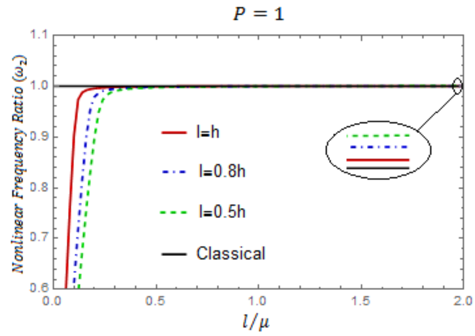

(b)

Fig. 6 Variation of (a) First and (b) Second nonlinear frequency ratio versus different length-scaled parameters of an FG DLNP. ($a_0/h = 0.5$)

Figs. 6(a) and 6(b) reveal the effect of different small length-scaled parameters on the nonlinear frequency ratio of FG DLNP.

$$\text{Nonlinear Frequency Ratio} = \frac{\text{nonlocal strain gradient nonlinear natural frequency}}{\text{Classical nonlinear natural frequency}} \quad (101)$$

It can be found from Fig. 6(a) that the nonlinear frequency ratio is smaller than 1 when $\mu > l$ and larger than 1 when $\mu < l$. These phenomena show that the FG DLNP reveals a stiffness-softening (nonlocal) when $\mu > l$, and reveals a stiffness-hardening (strain gradient) effect when $\mu < l$. It is clear that stiffness-hardening effect can be offset the stiffness-softening effect when $\mu = l$. The results of classical elasticity theory can be obtained by setting $\mu = 0$ and $l = 0$. It can be understood from Fig. 6(b) that when $\mu < l$ the effect of stiffness-hardening on frequency ratio of ω_2 is very low.

5.1 Influence of elastic foundation parameter on the dimensionless nonlinear frequency

The effects of the elastic foundation parameters on the nonlinear free vibration behavior of FG DLNP based on nonlocal strain gradient theory have been investigated in this study. Figs. 7-9 demonstrate the effects of the elastic foundation parameter on nonlinear frequency of simply supported FG DLNP. The following dimensionless foundation parameters $k_L a^4/D_1$, $k_s a^2/D_1$, $k_{NL} a^4 h^2/D_1$ and dimensionless natural frequency $\omega_{NL1} = \omega_1 a^2 \sqrt{\rho c * h/D_1^*}/\pi^2$ where $D_1^* = E_c h^3/(12(1-\nu^2))$are used in the plot of Figs. 7-9.

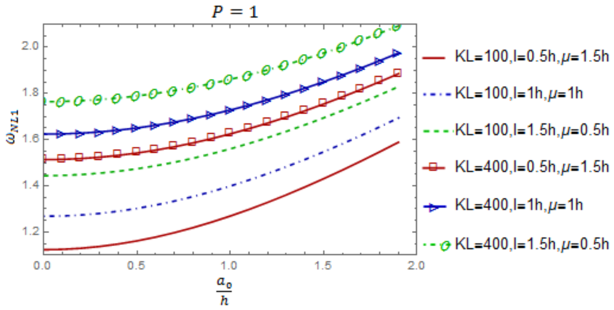

(a)

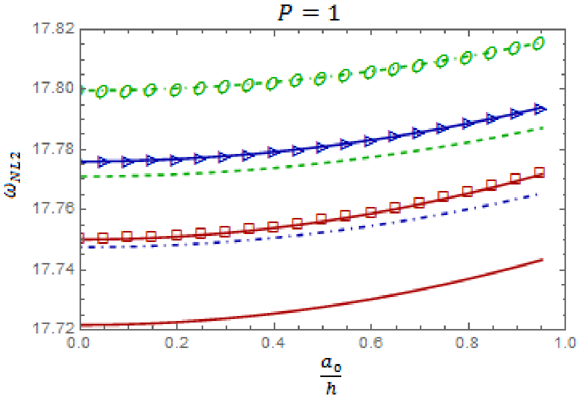

(b)

Fig. 7 Variation of the (a) First and (b) Second nonlinear frequency versus dimensionless amplitude for various Winkler foundation and length-scaled parameters of an FG DLNP

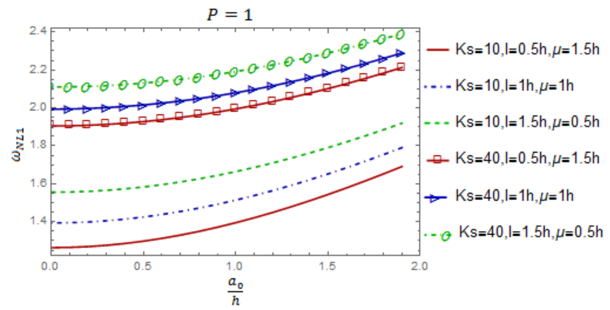

(a)

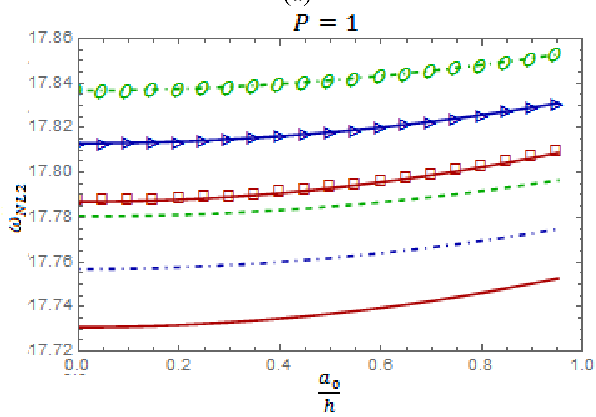

(b)

Fig. 8 Variation of the (a) First and (b) Second nonlinear frequency versus dimensionless amplitude for various Pasternak foundation and length-scaled parameters of an FG DLNP

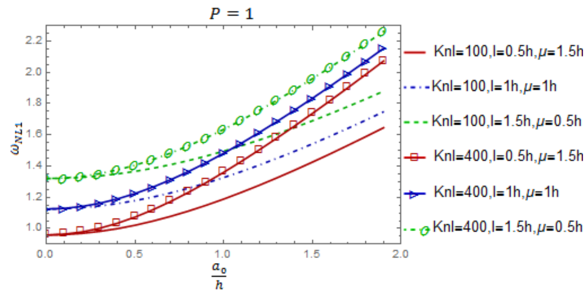

(a)

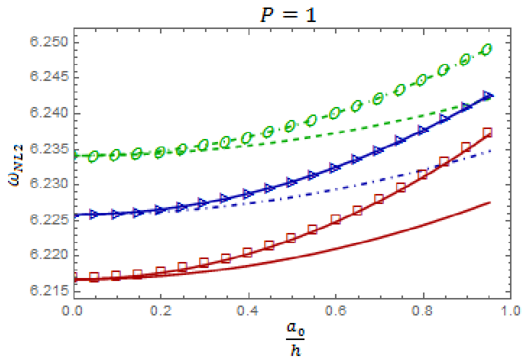

(b)

Fig. 9 Variation of the (a) First and (b) Second nonlinear frequency versus dimensionless amplitude for various nonlinear foundation and length-scaled parameters of an FG DLNP

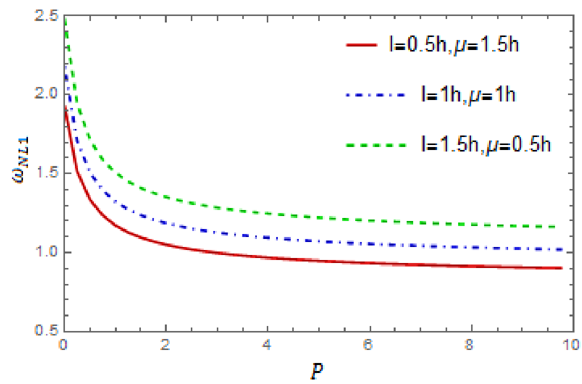

(a)

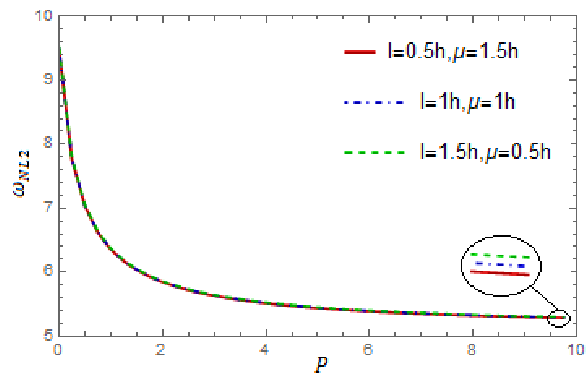

(b)

Fig. 10 Variations of the (a) First and (b) Second nonlinear dimensionless frequency versus the gradient index for the various length-scaled parameters of FG DLNP. ($a_0/h = 1$)

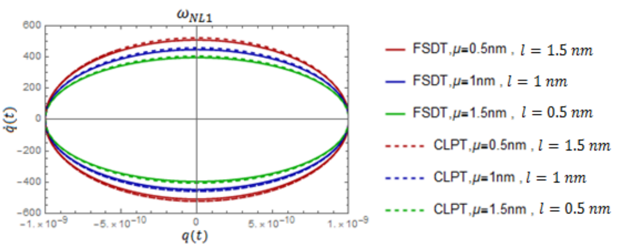

Fig. 11 Phase plane of the first nonlinear dimensionless frequency for the various length-scaled parameters of FG DLNP. ($a_0/h = 1$)

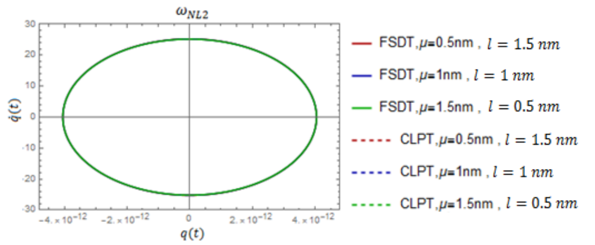

Fig. 12 Phase plane of the second nonlinear dimensionless frequency for the various length-scaled parameters of FG DLNP. ($a_0/h = 1$)

It can be seen from Fig. 7(a) that increasing the value of the linear elastic foundation parameter leads to increase in the nonlinear frequencies at a constant amplitude ratio. The linear elastic foundation parameter increases nanoplate stiffness and k_s and k_{NL} have a similar effect on nonlinear frequencies. The effects of linear and nonlinear elastic foundation on second nonlinear frequency are very low.

5.2 Influence of gradient index on the dimensionless nonlinear frequency

Variations of the first and second nonlinear dimensionless frequency of FG DLNP versus the gradient index based on nonlocal strain gradient theory are presented in Fig. 10 for various length-scaled parameters.

It can be seen from Fig. 10 that the first and second nonlinear dimensionless frequencies decrease with the increasing of the power law index P. Because, with the increasing of the power law index, the volume fraction of the softer and heavier material (SUS304) becomes larger, therefore the effective stiffness of the FG DLNP is decreased and the effective mass of the FG DLNP is increased. The effects of length scale parameters on second nonlinear frequency are very low.

5.3 Influence of small-scaled parameters on the phase plane

The significances of the small scale effects on phase plane diagrams ($\dot{q}(t)$ versus q(t)) of FG DLNP are investigated for the first and second nonlinear dimensionless frequency.

Fig. 11 displays that the phase plane diagrams for the first nonlinear dimensionless frequency of FG DLNP for the various length-scaled parameters. It is observed from Fig. 11 that the phase plane diagrams of FG DLNP in the presence of the small scale effect are symmetric ellipses. Fig. 11 exhibits that the area of the diagram becomes smaller by increasing the value of the nonlocal parameter and becomes greater by increasing the value of the strain gradient parameter. In other words, an increase/decrease in the area of the diagrams due to the mentioned parameters is equivalent to an increase/decrease in the initial velocity condition.

Fig. 12 displays the phase plane diagrams for the second nonlinear dimensionless frequency of FG DLNP for the various length-scaled parameters. It is observed from Fig. 12 that the area variations of the phase plane diagrams of FG DLNP remain almost unchanged.

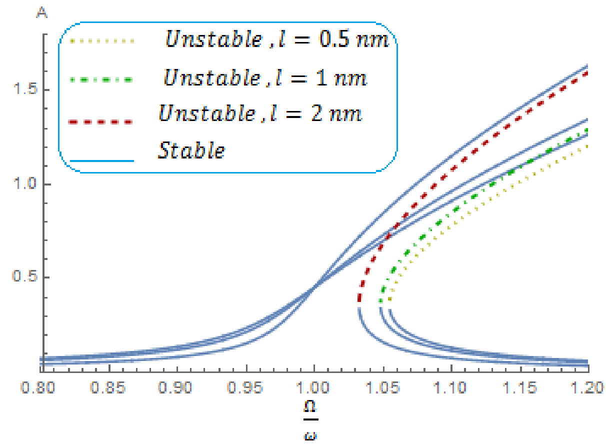

(a)

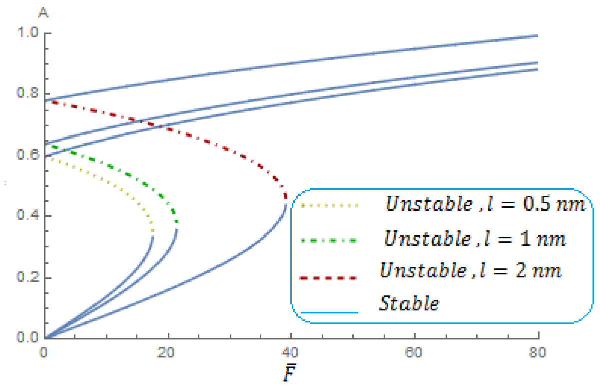

(b)

Fig. 13 Stable and unstable regions in a) Amplitude-frequency response excited in the vicinity of $\omega_{L1}$with $\bar{F} = 20$ and b) Amplitude of the response curves of the first and second layer sheets of DLNP.$\mu = 0.5\ nm$

5.4 Influence of small-scaled parameters on nonlinear forced vibration

The first and second layer of DLNP, the amplitude-frequency responses for external excitation are identical when the excited frequency is approaching to ω_{L1}= 0.1898 THz when $a = 10\ nm, b = 10\ nm, h = 1\ nm, E = 1.02\ TPa, \nu = 0.16$, $\rho = 2250\ kg/m^3$, $\mu = 0$ and $l = 0$. In other words, the first and second layers are vibrated in

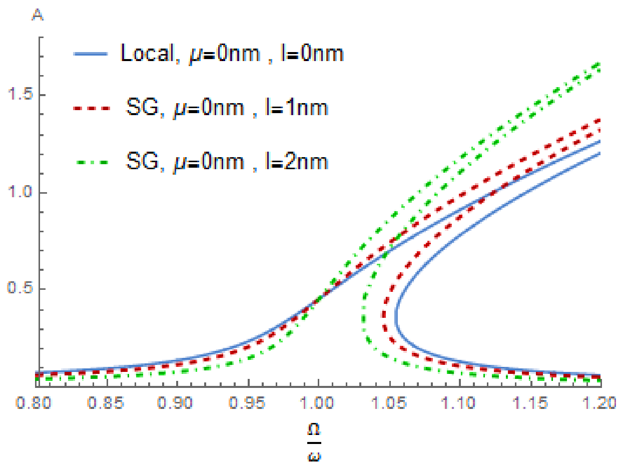

(a)

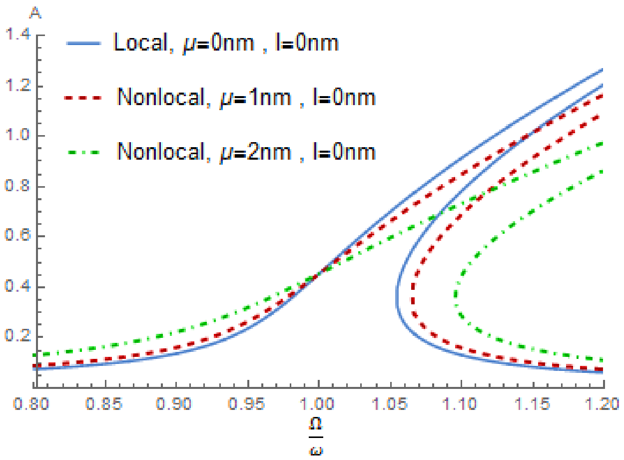

(b)

Fig. 14 Amplitude-frequency response curves of the first and second layer sheets of DLNP excited in the vicinity of ω_{L1} with $\bar{F} = 20$

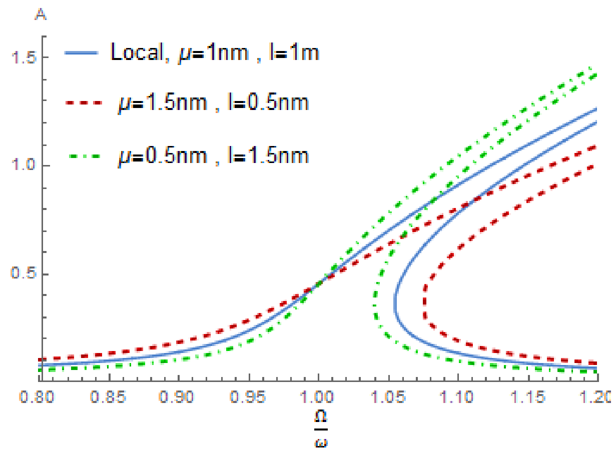

(a)

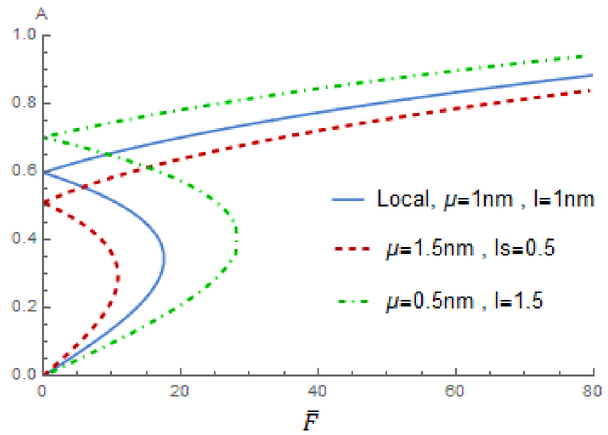

(b)

Fig. 15(a) Amplitude-frequency response excited in the vicinity of ω_{L1} with $\bar{F} = 20$ and b) Amplitude of the response curves of the first and second layer sheets of DLNP

phases in this spectrum of frequency.

Eq. (101) has two stable roots and an unstable root. Fig. 13 shows the stable and unstable regions.

It can be seen from Fig. 13(a) and 13(b) that increasing the material length scale parameter increases the width of unstable region.

It can be found from Fig. 14(a) and 14(b) that these curves give clearly nonlinearity of the hardening type, i.e. the response amplitude increases with increasing the frequency. Where A indicates the response amplitude of the first and second layer. The dimensionless force is defined as $\bar{F} = f_0\, a^4/(D \times h)$ where $D = Eh^3/(12(1-\nu^2))$. Fig. 14(a) shows that increasing the strain gradient parameter associated with the strain gradient (SG) theory causes to increasing the maximum response amplitude, whereas the increasing the nonlocal parameter causes to decreasing the maximum response amplitude (Fig. 14(b)).

Fig. 15(a) and 15(b) reveal the amplitude-frequency response and the amplitude of the response curves respectively.

It can be seen from Fig. 15 that when $\mu > l$ the amplitude of the response is smaller than classical elasticity theory and when $l > \mu$ is inverse.

6. Conclusions

In this study, the nonlinear free and forced vibration analysis of an FG DLNP embedded in an elastic medium was investigated based upon nonlocal strain gradient theory. The first order shear deformation plate theory was employed to model the nonlinear vibration of the FG DLNP. The properties of the plate were assumed to vary through the thickness of the plate with a power-law distribution. Due to introducing the physical neutral surface, there is no stretching-bending coupling in the size-dependent equations of motion of the FG DLNP. Explicit formulas are proposed for the first order shear deformation plate theory relevant to nonlocal strain gradient theory to evaluate the nonlinear natural frequencies and forced vibration of the FG DLNP. The semi-analytical solution for nonlinear natural frequencies using the Homotopy Analysis Method and the exact solution for nonlinear forced vibration through the Harmonic Balance method are obtained. The most concluding remarks are summarized as follows:

• The nonlinear natural frequencies can be generally increased with the increase of material length scale parameter or the decrease of nonlocal parameter.

• When the material length scale parameter is larger than the nonlocal parameter, the FG DLNP reveals a stiffness-hardening effect and the FG DLNP reveals a stiffness-softening effect, when the material length scale parameter is smaller than the nonlocal parameter.

• The increasing of elastic foundation parameters lead to increase in the nonlinear frequencies at a constant amplitude ratio and increasing in the material length scale parameter increases this effect.

• The nonlinear natural frequencies decrease with the increase of the power law index.

• Increasing the material length scale parameter increases the width of unstable region in the frequency response curve.

• The results show that the effects of maximum dimensionless amplitude, length scale parameters and gradient index on the second nonlinear frequency of FG DLNP are very low because the effect of vdW interaction force is very high.

• The length scale parameters give nonlinearity of the hardening type in frequency response curve and increasing the material length scale parameter causes to increased maximum response amplitude, whereas the increasing the nonlocal parameter causes to decreased maximum response amplitude.

• The phase plane diagrams of FG DLNP in the presence of the small scale effect are symmetric ellipses and the area of the diagram at the first frequency becomes smaller by increasing the value of the nonlocal parameter and becomes greater by increasing the value of the strain gradient parameter.

• The area variations of the phase plane diagrams for the second nonlinear dimensionless frequency of FG DLNP for the various length-scaled parameters remain almost unchanged.

References

Abdelaziz, H.H., Meziane, M.A.A., Bousahla, A.A., Tounsi, A., Mahmoud, S.R. and Alwabli, A.S. (2017), "An efficient hyperbolic shear deformation theory for bending, buckling and free vibration of FGM sandwich plates with various boundary conditions", *Steel Compos. Struct.*, **25**(6), 693-704.

Abualnour, M., Houari, M.S.A., Tounsi, A. and Mahmoud, S.R. (2018), "A novel quasi-3D trigonometric plate theory for free vibration analysis of advanced composite plates", *Compos. Struct.*, **184**, 688-697.

Ahouel, M., Houari, M.S.A., Bedia, E.A. and Tounsi, A. (2016), "Size-dependent mechanical behavior of functionally graded trigonometric shear deformable nanobeams including neutral surface position concept", *Steel Compos. Struct.*, **20**(5), 963-981.

Akgöz, B. and Civalek, Ö. (2011), "Buckling analysis of cantilever carbon nanotubes using the strain gradient elasticity and modified couple stress theories", *J. Comput. Theoret. Nanosci.*, **8**(9), 1821-1827.

Akgoz, B. and Civalek, O. (2011), "Nonlinear vibration analysis of laminated plates resting on nonlinear two-parameters elastic foundations", *Steel Compos. Struct.*, **11**(5), 403-421.

Akgoz, B. and Civalek, O. (2013), "Buckling analysis of linearly tapered micro-columns based on strain gradient elasticity", *Struct. Eng. Mech.*, **48**(2), 195-205.

Akgöz, B. and Civalek, Ö. (2016), "Bending analysis of embedded carbon nanotubes resting on an elastic foundation using strain gradient theory", *Acta Astronaut.*, **119**, 1-12.

Akgöz, B. and Civalek, Ö. (2017), "A size-dependent beam model for stability of axially loaded carbon nanotubes surrounded by Pasternak elastic foundation", *Compos. Struct.*, **176**, 1028-1038.

Akgöz, B. and Civalek, Ö. (2017), "Effects of thermal and shear deformation on vibration response of functionally graded thick composite microbeams", *Compos. Part B: Eng.*, **129**, 77-87.

Akhavan, H., Hashemi, S.H., Taher, H.R.D. Alibeigloo, A. and Vahabi, S. (2009), "Exact solutions for rectangular Mindlin plates under in-plane loads resting on Pasternak elastic foundation, Part I: Buckling analysis", *Comput. Mater. Sci.*, **44**(3), 968-978.

Alijani, F., Bakhtiari-Nejad, F. and Amabili, M. (2011), "Nonlinear vibrations of FGM rectangular plates in thermal environments", *Nonlin. Dyn.*, **66**(3), 251.

Apuzzo, A., Barretta, R., Canadija, M., Feo, L., Luciano, R. and Marotti de Sciarra, F. (2017a), "A closed-form model for torsion of nanobeams with an enhanced nonlocal formulation", *Compos. Part B*, **108**, 315-324.

Apuzzo, A., Barretta, R., Luciano, R., Marotti de Sciarra, F. and Penna, R. (2017b), "Free vibrations of Bernoulli-Euler nano-beams by the stress-driven nonlocal integral model", *Compos. Part B*, **123**, 105-111.

Askes, H. and Aifantis, E.C. (2011), "Gradient elasticity in statics and dynamics: an overview of formulations, length scale identification procedures, finite element implementations and new results", *Int. J. Sol. Struct.*, **48**(13), 1962-1990.

Barretta, R., Canadija, M., Feo, L., Luciano, R., Marotti de Sciarra, F. and Penna, R. (2018a), "Exact solutions of inflected functionally graded nano-beams in integral elasticity", *Compos. Part B*, **142**, 273-286.

Barretta, R., Canadija, M., Luciano, R. and Marotti de Sciarra, F. (2018b), "Stress-driven modeling of nonlocal thermoelastic behavior of nanobeams", *Int. J. Eng. Sci.*, **126**, 53-67.

Barretta, R., Diaco, M., Feo, L., Luciano, R., Marotti de Sciarra, F. and Penna, R. (2018c), "Stress-driven integral elastic theory for torsion of nano-beams", *Mech. Res. Commun.*, **87**, 35-41.

Barretta, R., Fabbrocino, F., Luciano, R. and Marotti de Sciarra, F. (2018f), "Closed-form solutions in stress-driven two-phase integral elasticity for bending of functionally graded nano-beams", *Phys. E*, **97**, 13-30.

Barretta, R., Faghidian, SA. and Luciano, R. (2018d), "Longitudinal Vibrations of NanoRods by StressDriven Integral Elasticity", *Mech. Adv. Mater. Struct.*, Accepted.

Barretta, R., Faghidian, SA., Luciano, R., Medaglia, CM. and Penna, R. (2018g), "Stress-driven two-phase integral elasticity for torsion of nano-beams", *Compos. Part B*, **145**, 62-69.

Barretta, R., Luciano, R., Marotti de Sciarra, F. and Ruta, G. (2018e), "Stress-driven nonlocal integral model for Timoshenko elastic nano-beams", *Eur. J. Mech. A. Sol.*, Accepted.

Bayat, M., Bayat, M. and Pakar, I. (2018), "Nonlinear vibration of oscillatory systems using semi-analytical approach", *Struct. Eng. Mech.*, **65**(4), 409-413.

Bayat, M., Bayat, M. and Pakar, I. (2014), "Forced nonlinear vibration by means of two approximate analytical solutions", *Struct. Eng. Mech.*, **50**(6), 853-862.

Belabed, Z., Houari, M.S.A., Tounsi, A., Mahmoud, S.R. and Bég, O.A. (2014), "An efficient and simple higher order shear and normal deformation theory for functionally graded material (FGM) plates", *Compos. Part B: Eng.*, **60**, 274-283.

Beldjelili, Y., Tounsi, A. and Mahmoud, S.R. (2016), "Hygro-thermo-mechanical bending of S-FGM plates resting on variable elastic foundations using a four-variable trigonometric plate theory", *Smart Struct. Syst.*, **18**(4), 755-786.

Belkorissat, I., Houari, M.S.A., Tounsi, A., Bedia, E.A. and Mahmoud, S.R. (2015), "On vibration properties of functionally graded nano-plate using a new nonlocal refined four variable model", *Steel Compos. Struct.*, **18**(4), 1063-1081.

Bellifa, H., Bakora, A., Tounsi, A., Bousahla, A.A. and Mahmoud, S.R. (2017), "An efficient and simple four variable refined plate theory for buckling analysis of functionally graded plates", *Steel Compos. Struct.*, **25**(3), 257-270.

Bellifa, H., Benrahou, K.H., Bousahla, A.A., Tounsi, A. and Mahmoud, S.R. (2017), "A nonlocal zeroth-order shear deformation theory for nonlinear postbuckling of nanobeams", *Struct. Eng. Mech.*, **62**(6), 695-702.

Bellifa, H., Benrahou, K.H., Hadji, L., Houari, M.S.A. and Tounsi, A. (2016), "Bending and free vibration analysis of functionally graded plates using a simple shear deformation theory and the concept the neutral surface position", *J. Brazil. Soc. Mech. Sci. Eng.*, **38**(1), 265-275.

Benchohra, M., Driz, H., Bakora, A., Tounsi, A., Bedia, E.A.A. and Mahmoud, S. (2018), "A new quasi-3D sinusoidal shear deformation theory for functionally graded plates", *Struct. Eng. Mech.*, **65**(1), 19-31.

Bennoun, M., Houari, M.S.A. and Tounsi, A. (2016), "A novel five-variable refined plate theory for vibration analysis of functionally graded sandwich plates", *Mech. Adv. Mater. Struct.*, **23**(4), 423-431.

Besseghier, A., Houari, M.S.A., Tounsi, A. and Mahmoud, S.R. (2017), "Free vibration analysis of embedded nanosize FG plates using a new nonlocal trigonometric shear deformation theory", *Smart Struct. Syst.*, **19**(6), 601-614.

Bouafia, K., Kaci, A., Houari, M.S.A., Benzair, A. and Tounsi, A. (2017), "A nonlocal quasi-3D theory for bending and free flexural vibration behaviors of functionally graded nanobeams", *Smart Struct. Syst.*, **19**(2), 115-126.

Bouderba, B., Houari, M.S.A., Tounsi, A. and Mahmoud, S.R. (2016), "Thermal stability of functionally graded sandwich plates using a simple shear deformation theory", *Struct. Eng. Mech.*, **58**(3), 397-422.

Bouhadra, A., Tounsi, A., Bousahla, A.A., Benyoucef, S. and Mahmoud, S.R. (2018), "Improved HSDT accounting for effect of thickness stretching in advanced composite plates", *Struct. Eng. Mech.*, **66**(1), 61-73.

Bounouara, F., Benrahou, K.H., Belkorissat, I. and Tounsi, A. (2016), "A nonlocal zeroth-order shear deformation theory for free vibration of functionally graded nanoscale plates resting on elastic foundation", *Steel Compos. Struct.*, **20**(2), 227-249.

Bourada, M., Kaci, A., Houari, M.S.A. and Tounsi, A. (2015), "A new simple shear and normal deformations theory for functionally graded beams", *Steel Compos. Struct.*, **18**(2), 409-423.

Bousahla, A.A., Benyoucef, S., Tounsi, A. and Mahmoud, S.R. (2016), "On thermal stability of plates with functionally graded coefficient of thermal expansion", *Struct. Eng. Mech.*, **60**(2), 313-335.

Bousahla, A.A., Houari, M.S.A., Tounsi, A. and Addabedia, E.A. (2014), "A novel higher order shear and normal deformation theory based on neutral surface position for bending analysis of advanced composite plates", *Int. J. Comput. Meth.*, **11**(6), 1350082.

Chaht, F.L., Kaci, A., Houari, M.S.A., Tounsi, A., Bég, O.A. and Mahmoud, S.R. (2015), "Bending and buckling analyses of functionally graded material (FGM) size-dependent nanoscale beams including the thickness stretching effect", *Steel Compos. Struct.*, **18**(2), 425-442.

Chen, W.J. and Li, X.P. (2013), "Size-dependent free vibration analysis of composite laminated Timoshenko beam based on new modified couple stress theory", *Arch. Appl. Mech.*, **83**(3), 431-444.

Civalek, Ö. (2013), "Nonlinear dynamic response of laminated plates resting on nonlinear elastic foundations by the discrete singular convolution-differential quadrature coupled approaches", *Compos. Part B: Eng.*, **50**, 171-179.

Civalek, Ö. and Demir, C. (2016), "A simple mathematical model of microtubules surrounded by an elastic matrix by nonlocal finite element method", *Appl. Math. Comput.*, **289**, 335-352.

Draiche, K., Tounsi, A. and Mahmoud, S.R. (2016), "A refined theory with stretching effect for the flexure analysis of laminated composite plates", *Geomech. Eng.*, **11**(5), 671-690.

Ebrahimi, F. and Barati, M.R. (2017), "Damping vibration analysis of smart piezoelectric polymeric nanoplates on viscoelastic substrate based on nonlocal strain gradient theory", *Smart Mater. Struct.*, **26**(6), 065018.

El-Haina, F., Bakora, A., Bousahla, A.A., Tounsi, A. and Mahmoud, S.R. (2017), "A simple analytical approach for thermal buckling of thick functionally graded sandwich plates", *Struct. Eng. Mech.*, **63**(5), 585-595.

Eringen, A.C. (1983), "On differential equations of nonlocal elasticity and solutions of screw dislocation and surface waves", *J. Appl. Phys.*, **54**(9), 4703-4710.

Faghidian, S.A. (2016), "Unified formulation of the stress field of Saint-Venant's flexure problem for symmetric cross-sections", *Int. J. Mech. Sci.*, **111-112**, 65-72.

Faghidian, S.A. (2017), "Unified formulations of the shear coefficients in Timoshenko beam theory", *J. Eng. Mech.*, **143**(9) 06017013-1:8.

Faghidian, S.A. (2018a), "On non-linear flexure of beams based on non-local elasticity theory", *Int. J. Eng. Sci.*, **124**, 49-63.

Faghidian, S.A. (2018b), "Reissner stationary variational principle for nonlocal strain gradient theory of elasticity", *Eur. J. Mech. A. Sol.*, **70**, 115-126.

Faghidian, S.A. (2018c), "Integro-differential nonlocal theory of elasticity", *Int. J. Eng. Sci.*, **129**, 96-110.

Gholami, R. and Ansari, R. (2017), "A unified nonlocal nonlinear higher-order shear deformable plate model for postbuckling analysis of piezoelectric-piezomagnetic rectangular nanoplates with various edge supports", *Compos. Struct.*, **166**, 202-218.

Gholami, R. and Ansari, R. (2018), "Grain size and nanoscale effects on the nonlinear pull-in instability and vibrations of electrostatic actuators made of nanocrystalline material", *Mater. Res. Expr.*, **5**(1), 015012.

Gürses, M., Civalek, Ö., Korkmaz, A.K. and Ersoy, H. (2009), "Free vibration analysis of symmetric laminated skew plates by discrete singular convolution technique based on first-order shear deformation theory", *Int. J. Numer. Meth. Eng.*, **79**(3), 290-313.

Haghani, A., Mondali, M. and Faghidian, S.A. (2018), "Linear and nonlinear flexural analysis of higher-order shear deformation laminated plates with circular delamination", *Acta Mech.*, **229**(4), 1631-1648.

Hamidi, A., Houari, M.S.A., Mahmoud, S.R. and Tounsi, A. (2015), "A sinusoidal plate theory with 5-unknowns and stretching effect for thermomechanical bending of functionally graded sandwich plates", *Steel Compos. Struct.*, **18**(1), 235-253.

He, X.Q., Wang, J.B., Liu, B. and Liew, K.M. (2012), "Analysis of nonlinear forced vibration of multi-layered graphene sheets". *Comput. Mater. Sci.*, **61**, 194-199.

Hebali, H., Tounsi, A., Houari, M.S.A., Bessaim, A. and Bedia, E.A.A. (2014), "New quasi-3D hyperbolic shear deformation theory for the static and free vibration analysis of functionally graded plates", *J. Eng. Mech.*, **140**(2), 374-383.

Hosseini-Hashemi, S., Fadaee, M. and Atashipour, S.R. (2011), "A new exact analytical approach for free vibration of Reissner-Mindlin functionally graded rectangular plates", *Int. J. Mech. Sci.*, **53**(1), 11-22.

Houari, M.S.A., Tounsi, A. and Bég, O.A. (2013), "Thermoelastic bending analysis of functionally graded sandwich plates using a new higher order shear and normal deformation theory", *Int. J. Mech. Sci.*, **76**, 102-111.

Houari, M.S.A., Tounsi, A., Bessaim, A. and Mahmoud, S.R. (2016), "A new simple three-unknown sinusoidal shear deformation theory for functionally graded plates", *Steel Compos. Struct.*, **22**(2), 257-276.

Huang, X.L. and Shen, H.S. (2004), "Nonlinear vibration and dynamic response of functionally graded plates in thermal environments", *Int. J. Sol. Struct.*, **41**, 2403-2427.

Jadhav, P.A. and Bajoria, K.M. (2013), "Free and forced vibration control of piezoelectric FGM plate subjected to electro-mechanical loading", *Smart Mater. Struct.*, **22**(6), 065021.

Jomehzadeh, E. and Saidi, A.R. (2011), "A study on large amplitude vibration of multilayered graphene sheets", *Comput. Mater. Sci.*, **50**(3), 1043-1051.

Karami, B., Janghorban, M. and Tounsi, A. (2017), "Effects of triaxial magnetic field on the anisotropic nanoplates", *Steel Compos. Struct.*, **25**(3), 361-374.

Karami, B., Janghorban, M. and Tounsi, A. (2018), "Nonlocal strain gradient 3D elasticity theory for anisotropic spherical nanoparticles", *Steel Compos. Struct.*, **27**(2), 201-216.

Karami, B., Janghorban, M. and Tounsi, A. (2018), "Variational approach for wave dispersion in anisotropic doubly-curved nanoshells based on a new nonlocal strain gradient higher order shell theory", *Thin-Wall. Struct.*, **129**, 251-264.

Kargarnovin, M.H., faghidian, S.A., Farjami, Y. and Farrahi, G.H. (2010), "Application of homotopy-padé technique in limit analysis of circular plates under arbitrary rotational Symmetric loading using von-mises yield criterion", *Commun. Nonlin. Sci. Numer. Simulat.*, **15**(4), 1080-1091.

Khaniki, H.B. and Hosseini-Hashemi, S. (2017), "Buckling analysis of tapered nanobeams using nonlocal strain gradient theory and a generalized differential quadrature method", *Mater. Res. Expr.*, **4**(6), 065003.

Khetir, H., Bouiadjra, M.B., Houari, M.S.A., Tounsi, A. and Mahmoud, S.R. (2017), "A new nonlocal trigonometric shear deformation theory for thermal buckling analysis of embedded nanosize FG plates", *Struct. Eng. Mech.*, **64**(4), 391-402.

Kitipornchai, S., He, X.Q. and Liew, K.M. (2005), "Continuum model for the vibration of multilayered graphene sheets", *Phys. Rev. B*, **72**(7), 075443.

Li, L. and Hu, Y. (2016), "Nonlinear bending and free vibration analyses of nonlocal strain gradient beams made of functionally graded material", *Int. J. Eng. Sci.*, **107**, 77-97.

Liao, S. (2012), "*Homotopy Analysis Method in Nonlinear Differential Equations*, Higher Education Press, Beijing, China.

Mahmoudpour, E., Hosseini-Hashemi, S.H. and Faghidian, S.A. (2018), "Non-linear vibration analysis of FG nano-beams resting on elastic foundation in thermal environment using stress-driven nonlocal integral model", *Appl. Math. Modell.*, **57**, 302-315.

Mehralian, F., Beni, Y.T. and Zeverdejani, M.K. (2017a), "Calibration of nonlocal strain gradient shell model for buckling analysis of nanotubes using molecular dynamics simulations", *Phys. B: Cond. Matt.*, **521**, 102-111.

Mehralian, F., Beni, Y.T. and Zeverdejani, M.K. (2017b), "Nonlocal strain gradient theory calibration using molecular dynamics simulation based on small scale vibration of nanotubes", *Phys. B: Cond. Matt.*, **514**, 61-69.

Mercan, K. and Civalek, Ö. (2016), "DSC method for buckling analysis of boron nitride nanotube (BNNT) surrounded by an elastic matrix", *Compos. Struct.*, **143**, 300-309.

Meziane, M.A.A., Abdelaziz, H.H. and Tounsi, A. (2014), "An efficient and simple refined theory for buckling and free vibration of exponentially graded sandwich plates under various boundary conditions", *J. Sandw. Struct. Mater.*, **16**(3), 293-318.

Mirzaei, M. and Kiani, Y. (2017), "Nonlinear free vibration of FG-CNT reinforced composite plates", *Struct. Eng. Mech.*, **64**(3), 381-390.

Mokhtar, Y., Heireche, H., Bousahla, A.A., Houari, M.S.A., Tounsi, A. and Mahmoud, S.R. (2018), "A novel shear deformation theory for buckling analysis of single layer graphene sheet based on nonlocal elasticity theory", *Smart Struct. Syst.*, **21**(4), 397-405.

Mouffoki, A., Bedia, E.A., Houari, M.S.A., Tounsi, A. and Mahmoud, S.R. (2017), "Vibration analysis of nonlocal advanced nanobeams in hygro-thermal environment using a new two-unknown trigonometric shear deformation beam theory", *Smart Struct. Syst.*, **20**(3), 369-383.

Qian, Y.H. and Zhang, Y.F. (2017), "Optimal extended homotopy analysis method for multi-degree-of-freedom nonlinear dynamical systems and its application", *Struct. Eng. Mech.*, **61**(1), 105-116.

Rajabi, K. and Hosseini-Hashemi, S. (2017), "Size-dependent free vibration analysis of first-order shear-deformable orthotropic nanoplates via the nonlocal strain gradient theory", *Mater. Res. Expr.*, **4**(7), 075054.

Shooshtari, A. and Khadem, S.E. (2006), "A multiple scales method solution for the free and forced nonlinear transverse vibrations of rectangular plates", *Struct. Eng. Mech.*, **24**(5), 543-560.

Sobhy, M. (2017), "Hygro-thermo-mechanical vibration and buckling of exponentially graded nanoplates resting on elastic foundations via nonlocal elasticity theory", *Struct. Eng. Mech.*, **63**(3), 401-415.

Wang, R.T. and Kuo, N.Y. (1999), "Nonlinear vibration of Mindlin plate subjected to moving forces including the effect of weight of the plate", *Struct. Eng. Mech.*, **8**(2), 151-164.

Wang, Y.Q. and Zu, J.W. (2017), "Porosity-dependent nonlinear forced vibration analysis of functionally graded piezoelectric smart material plates", *Smart Mater. Struct.*, **26**(10), 105014.

Wang, Y., Li, F., Jing, X. and Wang, Y. (2015), "Nonlinear vibration analysis of double-layered nanoplates with different boundary conditions", *Phys. Lett. A*, **379**(24-25), 1532-1537.

Yazid, M., Heireche, H., Tounsi, A., Bousahla, A.A. and Houari, M.S.A. (2018), "A novel nonlocal refined plate theory for stability response of orthotropic single-layer graphene sheet resting on elastic medium", *Smart Struct. Syst.*, **21**(1), 15-25.

Youcef, D.O., Kaci, A., Benzair, A., Bousahla, A.A. and Tounsi, A. (2018), "Dynamic analysis of nanoscale beams including surface stress effects", *Smart Struct. Syst.*, **21**(1), 65-74.

Younsi, A., Tounsi, A., Zaoui, F.Z., Bousahla, A.A. and Mahmoud, S.R. (2018), "Novel quasi-3D and 2D shear deformation theories for bending and free vibration analysis of FGM plates", *Geomech. Eng.*, **14**(6), 519-532.

Zemri, A., Houari, M.S.A., Bousahla, A.A. and Tounsi, A. (2015), "A mechanical response of functionally graded nanoscale beam: an assessment of a refined nonlocal shear deformation theory beam theory", *Struct. Eng. Mech.*, **54**(4), 693-710.

Zhao, Y.B., Sun, C.S., Wang, Z.Q. and Peng, J. (2014), "Nonlinear in-plane free oscillations of suspended cable investigated by homotopy analysis method", *Struct. Eng. Mech.*, **50**(4), 487-500.

Zidi, M., Houari, M.S.A., Tounsi, A., Bessaim, A. and Mahmoud, S.R. (2017). "A novel simple two-unknown hyperbolic shear deformation theory for functionally graded beams", *Struct. Eng. Mech.*, **64**(2), 145-153.

Zidi, M., Tounsi, A., Houari, M.S.A. and Bég, O.A. (2014), "Bending analysis of FGM plates under hygro-thermo-mechanical loading using a four variable refined plate theory", *Aerosp. Sci. Technol.*, **34**, 24-34.

PL

Appendix

$$N_i^* = N_i - \frac{D_1}{\kappa^2 \nu_1 B_1}\nabla^2 N_i + \frac{m_2}{\kappa^2 \nu_1 B_1}(1-\mu^2\nabla^2)\ddot{N}_i \quad ,i=1,2$$
$$f_i^* = q_i - \frac{D_1}{\kappa^2 \nu_1 B_1}\nabla^2 q_i + \frac{m_2}{\kappa^2 \nu_1 B_1}(1-\mu^2\nabla^2)\ddot{q}_i \quad ,i=1,2$$
$$C_i^* = C_i - \frac{cD_1}{\kappa^2 \nu_1 B_1}\nabla^2 C_i + \frac{m_2}{\kappa^2 \nu_1 B_1}(1-\mu^2\nabla^2)\ddot{C}_i, \quad i=1,2$$
$$N_i = \frac{\partial^2 \phi_i}{\partial y^2}\frac{\partial^2 w_i}{\partial x^2} + \frac{\partial^2 \phi_i}{\partial x^2}\frac{\partial^2 w_i}{\partial y^2} - 2\frac{\partial^2 \phi_i}{\partial x \partial y}\frac{\partial^2 w_i}{\partial x \partial y}, \quad i=1,2$$
$$C_1 = c(w_1 - w_2) \quad , \quad C_2 = c(w_2 - w_1)$$
$$q_1 = F(x,y,t) - k_l w_1 - k_{nl} {w_1}^3 + k_s \nabla^2 w_1$$
$$q_2 = -k_l w_2 - k_{nl} {w_2}^3 + k_s \nabla^2 w_2 \tag{A.1}$$

$$E_3 = -\frac{a_0^3 \omega_2^6((\beta_3+\beta_4)\omega_1^2 - \beta_5)}{4(\omega_1^2-\omega_2^2)^3}$$
$$E_4 = \frac{a_0^3 \omega_1^6((\beta_3+\beta_4)\omega_2^2 - \beta_5)}{4(\omega_1^2-\omega_2^2)^3}$$
$$E_5 = -\frac{a_0^3 \omega_2^2 \omega_1^4(-3\beta_5 + \beta_3\omega_1^2 + (2\beta_3+\beta_4)\omega_2^2 - 2\beta_4\omega_1\omega_2)}{4(\omega_1^2-\omega_2^2)^3}$$
$$E_6 = \frac{a_0^3 \omega_2^4 \omega_1^2(-3\beta_5 + \beta_3\omega_2^2 + (2\beta_3+\beta_4)\omega_1^2 - 2\beta_4\omega_1\omega_2)}{4(\omega_1^2-\omega_2^2)^3}$$
$$E_7 = -\frac{a_0^3 \omega_2^2 \omega_1^4(-3\beta_5 + \beta_3\omega_1^2 + (2\beta_3+\beta_4)\omega_2^2 + 2\beta_4\omega_1\omega_2)}{4(\omega_1^2-\omega_2^2)^3}$$
$$E_8 = \frac{a_0^3 \omega_2^4 \omega_1^2(-3\beta_5 + \beta_3\omega_2^2 + (2\beta_3+\beta_4)\omega_1^2 + 2\beta_4\omega_1\omega_2)}{4(\omega_1^2-\omega_2^2)^3} \tag{A.2}$$

$$H_1 = \frac{1}{\omega_1^2-\omega_2^2}[(H_3+H_4+H_5+H_6+H_7+H_8)\omega_2^2 - 9\omega_1^2 H_3 - 9\omega_2^2 H_4 - (\omega_1-2\omega_2)^2 H_5 - (\omega_1+2\omega_2)^2 H_6 - (2\omega_1-\omega_2)^2 H_7 - (2\omega_1+\omega_2)^2 H_8]$$
$$H_2 = \frac{1}{\omega_2^2-\omega_1^2}[(H_3+H_4+H_5+H_6+H_7+H_8)\omega_1^2 - 9\omega_1^2 H_3 - 9\omega_2^2 H_4 - (\omega_1-2\omega_2)^2 H_5 - (\omega_1+2\omega_2)^2 H_6 - (2\omega_1-\omega_2)^2 H_7 - (2\omega_1+\omega_2)^2 H_8]$$
$$H_3 = \frac{E_3}{8\omega_1^2(9\omega_1^2-\omega_2^2)}$$
$$H_4 = \frac{E_4}{8\omega_2^2(9\omega_2^2-\omega_1^2)}$$
$$H_5 = \frac{E_5}{(\omega_1-2\omega_2)^4 - (\omega_1^2+\omega_2^2)(\omega_1-2\omega_2)^2 + (\omega_1\omega_2)^2}$$
$$H_6 = \frac{E_6}{(\omega_1+2\omega_2)^4 - (\omega_1^2+\omega_2^2)(\omega_1+2\omega_2)^2 + (\omega_1\omega_2)^2}$$
$$H_7 = \frac{E_7}{(2\omega_1-\omega_2)^4 - (\omega_1^2+\omega_2^2)(2\omega_1-\omega_2)^2 + (\omega_1\omega_2)^2}$$
$$H_8 = \frac{E_8}{(2\omega_1+\omega_2)^4 - (\omega_1^2+\omega_2^2)(2\omega_1+\omega_2)^2 + (\omega_1\omega_2)^2} \tag{A.3}$$